NASA TECHNICAL NOTE

NASA TN D-5294

NASA TN D-5294

FATIGUE OF NOTCHED Ti-8Al-1Mo-1V TITANIUM ALLOY AT ROOM TEMPERATURE AND 550° F (560° K) WITH FLIGHT-BY-FLIGHT LOADING REPRESENTATIVE OF A SUPERSONIC TRANSPORT

by L. A. Imig and Walter Illg

Langley Research Center
Langley Station, Hampton, Va.

NATIONAL AERONAUTICS AND SPACE ADMINISTRATION • WASHINGTON, D. C. • JULY 1969

NASA TN D-5294

FATIGUE OF NOTCHED Ti-8Al-1Mo-1V TITANIUM ALLOY AT ROOM TEMPERATURE AND 550° F (560° K) WITH FLIGHT-BY-FLIGHT LOADING REPRESENTATIVE OF A SUPERSONIC TRANSPORT

By L. A. Imig and Walter Illg

Langley Research Center
Langley Station, Hampton, Va.

NATIONAL AERONAUTICS AND SPACE ADMINISTRATION

For sale by the Clearinghouse for Federal Scientific and Technical Information
Springfield, Virginia 22151 – CFSTI price $3.00

FATIGUE OF NOTCHED Ti-8Al-1Mo-1V TITANIUM ALLOY AT ROOM TEMPERATURE AND 550° F (560° K) WITH FLIGHT-BY-FLIGHT LOADING REPRESENTATIVE OF A SUPERSONIC TRANSPORT

By L. A. Imig and Walter Illg
Langley Research Center

SUMMARY

Fatigue studies were conducted on notched sheet specimens of Ti-8Al-1Mo-1V titanium alloy. The effects of loading parameters and elevated temperature on fatigue life were investigated in variable-amplitude tests that simulated flight loading of a supersonic transport operating at a Mach number of 3. Test stresses were applied flight by flight either at room temperature or at 550° F (560° K). Test results indicated a strong influence of design mean stress, the ground-air-ground cycle, and elevated temperature. Effects due to simulated taxi stresses and thermal stresses were observed to be small. A series of constant-amplitude tests on the same type of specimen that was used in the variable-amplitude tests was conducted to provide data for a linear cumulative-damage analysis.

INTRODUCTION

The fatigue resistance of supersonic-transport structural material depends on the effect of elevated temperature on structural resistance to service loads. A knowledge of the interactions of temperature and loading is valuable for guidance in formulating test programs as well as structural design for prototype supersonic transports.

Accordingly, in the present investigation, the influences of the design mean stress, the minimum stress for ground-air-ground cycles, taxi stresses, and thermal stresses were investigated for simulated operational and check flights. Stresses that were representative of those at a critical station in the tension surface of a wing were applied in flight-by-flight (variable-amplitude) fatigue tests at room temperature and 550° F (560° K). The flight-by-flight method of testing was selected, because previous research (refs. 1 and 2) has shown fatigue life to be affected by simplification of the expected service-load experience. The elevated-temperature tests were conducted at 550° F (560° K), because that temperature was considered to be representative of the equilibrium skin temperature for flight at a Mach number of 3. Studies were conducted at values of

design mean stress that ranged upward from the approximate value of design mean stress expected in an operating supersonic airplane made of titanium. The studies were conducted on notched sheet specimens of duplex-annealed Ti-8Al-1Mo-1V titanium alloy. The results of the variable-amplitude tests were analyzed according to the linear cumulative-damage concept. The analysis was based on the results of constant-amplitude fatigue tests at room temperature and 550° F (560° K) on specimens similar to those used in the variable-amplitude tests.

SYMBOLS

The units used for the physical quantities defined in this paper are given both in the U.S. Customary Units and in the International System of Units (SI). Factors relating these two systems of units are given in reference 3, and those pertinent to the present investigation are presented in appendix A.

A surface area of wing, ft^2 (m^2)

a rate of change of lift coefficient with respect to angle of attack, 1/radian

a_n vertical acceleration divided by acceleration due to gravity

$\bar{c}$ mean geometric chord, ft (m)

F function of airplane characteristics, $\frac{U_{de}}{\theta}$, ft/sec (m/sec)

g acceleration due to gravity, 32.2 ft/sec^2 (9.81 m/sec^2)

K_g gust alleviation factor, $\frac{0.88\mu_g}{5.3 + \mu_g}$

K_T theoretical elastic-stress concentration factor

k_1, k_2, P_1, P_2 turbulence factors

m instantaneous gross mass of airplane, slugs (kg)

m_d design gross mass of airplane, slugs (kg)

$m^* = \frac{m}{m_d} = \frac{S_{1g}}{S_{1g,d}}$

N	number of stress cycles required to cause failure at given stress level
n	number of stress cycles applied at given stress level
$\sum \frac{n}{N}$	life fraction at failure for tests at more than one stress level
r	radius, in. (m)
S	stress, ksi (N/m^2)
S_{1g}	stress during level unaccelerated flight, ksi (N/m^2)
$S_{1g,d}$	design mean stress (stress during level unaccelerated flight at maximum gross mass), ksi (N/m^2)
ΔS	stress amplitude, ksi (N/m^2)
U_{de}	derived gust velocity, ft/sec (m/sec)
V	true airplane velocity, knots (m/sec)
V_e	equivalent airplane velocity, $V\sqrt{\rho/\rho_o}$, knots (m/sec)
θ	ratio of stress amplitude to design mean stress, $\frac{\Delta S}{S_{1g,d}}$
μ_g	airplane mass ratio, $\frac{2m}{\rho \bar{c} a A}$
ρ	mass density of air, slugs/ft^3 (kg/m^3)
ρ_o	standard mass density of dry air at sea level, 0.002378 slug/ft^3 (1.22557 kg/m^3)

Subscripts:

max	maximum
mean	mean
min	minimum

SCOPE OF INVESTIGATION

Specimens

Specimens were made from duplex-annealed Ti-8Al-1Mo-1V titanium-alloy sheet and were 0.050 inch (1.27 mm) thick. The sheets were rolled from three heats of material. The chemical composition of each heat, as determined by the manufacturer, is presented in table I. The longitudinal tensile properties, as determined from standard tensile tests, are shown in table II. The machining details for manufacture of the fatigue specimens, shown in figure 1, are given in appendix B. The fatigue specimens had a theoretical elastic-stress concentration factor K_T of 4 and represented a structural region containing a moderate stress concentration. Similar specimens were used in previous research at the Langley Research Center for investigations of aluminum alloys, because they were shown (ref. 4) to approximate the fatigue behavior of various aluminum structures and components. The specimens were tested under constant- and variable-amplitude loading applied axially at room temperature and 550° F (560° K). The temperature was maintained at a constant level throughout elevated-temperature tests. In general, at least three tests were conducted for each test condition. Details of the procedures for the tensile, variable-amplitude, and constant-amplitude tests are presented in appendix B.

Parameters for Variable-Amplitude Fatigue Tests

Loads due to atmospheric turbulence were derived from a mathematical model of the atmosphere and were used in conjunction with an assumed vehicle. Maneuver loads based on data from current subsonic airplanes and the derived gust loads were used to form the spectrum of stresses. In variable-amplitude fatigue tests, stresses were programed to simulate individual flights. The detailed methods by which the loading statistics were derived and separated into flights are presented in appendix C.

The flights were of two kinds: operational and check flights. Operational flying as used herein means the use of an airplane for routine commercial operation. Check flying means the use of an airplane for other than routine operation and usually denotes flights for crew training. The stress sequence for operational flights presented in figure 2(a) shows the true number of cycles applied. The three most prominent aspects of the stress history for operational flights are (1) more stress cycles occurred during climb than during cruise or descent, (2) the mean stress decreased throughout the flight to simulate a loss of mass due to fuel usage, and (3) a compressive stress that completed the ground-air-ground (GAG) transition occurred at the end of the flight. Stresses for all tests were applied as rapidly as the testing equipment would permit; flights of the type shown in figure 2(a) were completed in about 5 seconds.

Flights containing the number of stress cycles shown in figure 2(a) are called basic operational flights. More severe stresses that occurred less frequently than once per flight were added to those shown in figure 2(a) at times representing fifth, 100th, 1000th, and 10 000th flights. This approach led to flights of differing severity; the 10 000th flight was the most severe, and it is shown in figure 2(b). Check flights, represented in figure 2(c), had a mean stress of $0.7S_{1g,d}$ and were applied after every 24 operational flights. Seven GAG cycles were included in each check flight to represent touch-and-go landings that occur frequently during check flights. Infrequently occurring severe stresses were added to every 10th and 100th check flight. The same sequence of check flights was applied in all variable-amplitude fatigue tests. The following paragraphs describe the parameters that were varied in the operational flights.

Design mean stress (type A tests).- For type A tests, the sequences of stresses for operational flights shown in figure 2 were applied with design mean stresses $S_{1g,d}$ of 25, 30, and 35 ksi (170, 210, and 240 MN/m^2). The results from all other types of tests were compared with those from type A tests. The stress sequences used for other types of tests are shown schematically in figure 3. The boxes in the figure represent the stress cycles for the basic flight and are identified by letter according to the type of test to which they correspond.

Taxi stresses (type B tests).- As indicated in figure 3, type B tests included stress cycles at the end of each flight to represent stresses induced by travel along taxiways. Taxi stresses were represented by one stress cycle in each basic flight. Fifth, 100th, 1000th, and 10 000th flights, which contained more flight stresses, also contained more than one taxi stress cycle. The minimum stress for taxi stress cycles was $-0.5S_{1g,d}$.

Thermal stresses (type C and D tests).- Thermal stress occurs in a structure when aerodynamic heating causes temperature gradients between the interior and exterior structure. A tensile thermal stress develops internally while the airplane is heating and a compressive thermal stress develops internally while the airplane is cooling. This thermal stress cycle was simulated by adding a stress of $0.6S_{1g,d}$ to the mean stress for cruise and by subtracting a stress of $0.4S_{1g,d}$ from the mean stress for descent as shown in figure 3 by the positions of the boxes labeled C. Tests with this thermal cycle were called type C.

The opposite thermal stress cycle, for the exterior structure, was simulated by subtracting a stress of $0.6S_{1g,d}$ from the mean stress for cruise and by adding a stress of $0.4S_{1g,d}$ to the mean stress for descent. This thermal stress cycle is represented in figure 3 by the positions of the boxes labeled D.

GAG stress range (type E tests).- The GAG stress range was represented by two series of tests, both designated type E. The sequence of flight stresses used for the two kinds of type E tests was identical to that for type A tests except that in one type E test

the minimum stress for GAG cycles was zero ($\theta_{min} = 0$) and in the other the minimum stress was $-S_{1g,d}$ ($\theta_{min} = -1$). All type E tests were conducted at a design mean stress of 30 ksi (210 MN/m^2).

RESULTS AND DISCUSSION

Tensile Tests

The longitudinal tensile properties of the material used in this investigation are presented in table II and are considered to be typical of this titanium alloy. Representative stress-strain curves obtained in tests at room temperature and 550° F (560° K) are presented in figure 4. The yield strength of the material is considerably lower at 550° F (560° K) than at room temperature as indicated by the figure. The difference between the strengths at room temperature and elevated temperature is comparable to that reported in reference 5 for similar material.

Variable-Amplitude Fatigue Tests

Fatigue lives are presented in tables III and IV for variable-amplitude tests at room temperature and at 550° F (560° K), respectively, and are plotted in figure 5. The fatigue lives are the total number of flights (operational and check) that were survived by test specimens before complete failure occurred. The lengths of the bars in figure 5 indicate the geometric mean lives of all failures for a particular test condition. If failure had not occurred and no fatigue cracks had initiated in 52 000 flights, tests were terminated, and lives for those specimens were not included in the calculation of the geometric mean life. Such tests are indicated by an arrowhead at the end of a bar in figure 5; the number of such tests is indicated by the numerals in the arrowhead.

The stress level at which failure occurred, the segment of flight in which failure occurred, and the kind of flight in which failure occurred are also presented in tables III and IV. Most of the test specimens failed during the climb segment of the flight. The only exceptions were in tests with simulated thermal stress for the interior structure (type C) in which some failures occurred during cruise. Maximum nominal stresses were higher during cruise in basic flights, fifth flights, and 100th flights for type C tests relative to type A tests; consequently, all the failures during cruise occurred in basic, fifth, or 100th flights.

Test results indicated a strong influence of the design mean stress and the minimum stress for ground-air-ground cycles. Effects due to simulated taxiing and thermal stresses were small. In general, fatigue lives for elevated-temperature tests were approximately half those for room-temperature tests.

Effect of design mean stress (type A tests).- As expected, tests at higher design mean stresses produced shorter fatigue lives than those at lower design mean stresses as shown in figure 5. The effect of design mean stress was approximately the same in tests at both temperatures.

Effect of minimum stress for GAG cycles (type E tests).- All type E tests were conducted at a value of $S_{1g,d}$ of 30 ksi (210 MN/m^2). Fatigue lives from tests in which the minimum stress for the GAG cycle was $-S_{1g,d}$ ($\theta_{min} = 1$) were about one-fifth those from tests in which the minimum stress was zero ($\theta_{min} = 0$). (See fig. 5.) The main reason for the large differences in fatigue life in these tests is that the total stress range was much larger for tests with a minimum stress of $-S_{1g,d}$ than for tests with a minimum stress of zero. The present results indicate that the effect of GAG cycles on the life of notched titanium is similar in magnitude to that reported in reference 2 for notched specimens of 7075-T6 aluminum alloy.

Effect of taxi stresses (type B tests).- Taxi stresses had little effect except in tests at 25 ksi (170 MN/m^2) as shown in figure 5. For those tests, the taxi stresses produced failure in two of the three room-temperature tests whereas no failures occurred in the reference tests (type A); a similar but less significant effect of the taxi stresses occurred in tests at 550° F (560° K).

Effect of thermal stresses (type C and D tests).- Both types of thermal stress caused shorter fatigue lives than the reference tests; however, thermal stress for the interior structure (type C) produced larger differences from the reference fatigue lives than did thermal stress for the exterior structure (type D) – particularly in tests at the lowest design mean stress. The shorter lives for type C tests were undoubtedly due to the higher maximum stresses that occurred during cruise in basic, fifth, and 100th flights. In tests with thermal stress for the exterior structure (type D), differences from the reference fatigue lives were not clearly enough established to be considered significant.

Constant-Amplitude Fatigue Tests

Constant-amplitude fatigue data are presented in table V for tests at room temperature and in table VI for tests at 550° F (560° K). Plots of maximum stress as a function of the number of cycles required for failure are presented in figure 6. The figure presents the results of tests at room temperature and 550° F (560° K) for mean stresses of -15, 0, 25, and 50 ksi (-100, 0, 170, and 350 MN/m^2). The symbols on the figure are plotted at the geometric mean life of all specimens that failed at a particular stress level. The scatter band at each stress level extends to the maximum and minimum lives. In cases for which no scatter band is shown, the symbol covers the range of scatter. The curves were faired through the geometric mean lives.

The effects of the elevated temperature depended on the mean stress; at the two lowest mean stresses, the fatigue limits for elevated-temperature tests were lower than those for room-temperature tests, but at higher mean stresses, the fatigue limits for elevated-temperature tests were higher than those for room-temperature tests. Other cases in which the fatigue limits at elevated temperature were higher than those at room temperature were reported in references 6 to 8; thus, such behavior is not uncommon.

Although the reasons that the fatigue limits at elevated temperature were higher than those at room temperature are not completely understood, consideration of the local stresses and strains at the notch roots leads to conclusions that are consistent with the test results. As mentioned earlier, the material has a lower yield strength at 550° F (560° K) than at room temperature; therefore, in tests at a nominal stress level sufficiently high to cause local yielding, the maximum local stress at the notch roots was lower at elevated temperature than at room temperature. Because the alternating stresses were equal and elastic in tests at both temperatures for a given nominal stress level, the local mean stress was lower in elevated-temperature tests than in room-temperature tests. Thus, specimens in the elevated-temperature tests could be expected to have longer lives than specimens in the room-temperature tests for the case of high mean stresses and low alternating stresses (near the fatigue limit). For short lives, the lower ultimate strength at elevated temperature relative to that at room temperature apparently became the predominant factor, because the fatigue lives at elevated temperature were observed to be shorter than those at room temperature.

An argument, converse to that applied in the preceding paragraph for the case of high mean stresses, may be made for the tests at a mean stress of -15 ksi (-100 MN/m^2) by assuming that the compressive stress-strain curves are similar to the tensile stress-strain curves. For the tests at a mean stress of -15 ksi (-100 MN/m^2), the minimum nominal stress was low enough to cause compressive yielding that resulted in higher mean and maximum local stresses at the notch roots. Therefore, the fatigue lives should have been shorter in the elevated-temperature tests than in the room-temperature tests as was observed.

For the case in which the nominal mean stress was zero, the local mean stress probably remained at zero throughout the tests. At a given nominal stress level, larger local strains would have occurred in the elevated-temperature tests than in the room-temperature tests, and shorter fatigue lives should have resulted as was observed. Thus, the observed effects of elevated temperature on constant-amplitude fatigue life can be qualitatively explained by considering the local stresses and strains at the notch roots.

The curves of maximum stress as a function of fatigue life in figure 6 were used to construct the plots of alternating stress as a function of mean stress shown in figures 7 and 8 for room temperature and 550° F (560° K), respectively. These curves

identify the combinations of mean and alternating stress that produce constant fatigue lives and were used as the basis for calculating fatigue damage.

Cumulative-Damage Analysis

Miner's method (ref. 9) was used to estimate cumulative damage from variable-amplitude tests because of its simplicity and wide use by other investigators. Life fractions (values of n/N) were calculated for each combination of alternating and mean stress for each test condition. The stress range for the GAG cycle was assumed to be from the minimum to the maximum stress occurring in a given flight.

The values of $\sum \frac{n}{N}$ at failure calculated for each type of test are presented in table VII. The tabulations indicate that the fatigue lives calculated by this method were overestimated if it is assumed that $\sum \frac{n}{N} = 1$ at failure. The present results are consistent with the results of reference 2 in which $\sum \frac{n}{N}$ at failure was also less than 1 for tests with GAG cycles extending into compression. The tabulations indicate that GAG cycles were the predominant source of damage; even so, on the basis of the data in figures 7 and 8, it is apparent that tests conducted only with GAG cycles would produce longer fatigue lives than the present tests which included flight stresses. The tabulations also indicate that check flights contributed very little to the calculated damage. References 10 to 12 indicate that check-flight maneuvers produce accelerations to a given level in fewer flight miles than either gusts or operational-flight maneuvers. From that information, the conclusion might be made that check flights are a major source of fatigue damage. However, in the present investigation, check flights had lower stresses at 1g than operational flights and constituted only 4 percent of the total number of flights. Thus, the calculated damage due to check flights was small for this investigation.

CONCLUSIONS

This investigation has been conducted to determine the relative importance of some of the loading parameters that might influence the fatigue life of structural material in supersonic airplanes. The investigation was conducted on notched sheet specimens of duplex-annealed Ti-8Al-1Mo-1V titanium alloy. Loads due to atmospheric turbulence were derived from a mathematical model of the atmosphere and were used in conjunction with an assumed vehicle. Maneuver loads based on data from current subsonic airplanes and the derived gust loads were used to form the spectrum of stresses. Parameters investigated included design mean stress, elevated temperature, the stress range associated with the ground-air-ground cycle, taxi stress, and thermal stress. The results of the investigation support the following conclusions:

1. The design mean stress and the minimum stress for ground-air-ground cycles had the greatest effects on fatigue life in tests that simulated airplane operation.

2. Simulated taxiing and thermal stresses had little effect on fatigue life; however, thermal stress for the interior structure produced specimen failures during the cruise segment of flight whereas all other test conditions produced specimen failures during the climb segment of flight.

3. Variable-amplitude fatigue lives from tests at 550° F (560° K) were approximately half as long as the lives from tests at room temperature for all test conditions.

4. Constant-amplitude fatigue lives were shorter at 550° F (560° K) than at room temperature in tests conducted at low mean stresses. In tests at high mean stresses and with maximum stresses near the fatigue limit, the fatigue lives were longer at 550° F (560° K) than at room temperature.

Langley Research Center,
National Aeronautics and Space Administration,
Langley Station, Hampton, Va., April 10, 1969,
129-03-06-04-23.

APPENDIX A

CONVERSION OF U.S. CUSTOMARY UNITS TO THE INTERNATIONAL SYSTEM OF UNITS

The International System of Units (SI) was adopted by the Eleventh General Conference on Weights and Measures, Paris, 1960. (See ref. 3.) Conversion factors for the units used in this report are taken from reference 3 and are presented in the following table:

Physical quantity	U.S. Customary Unit	Conversion factor (*)	SI Unit (**)
Length	in.	0.0254	meters (m)
Temperature	^{o}F	$\frac{5}{9}(^{o}F + 459.67)$	degrees Kelvin (^{o}K)
Force	lbf	4.448	newtons (N)
Stress	ksi = 1000 lbf/in^2	6.895×10^6	newtons/$meter^2$ (N/m^2)
Mass	slugs	14.59	kilograms (kg)
Density	$slugs/ft^3$	515.38	kilograms/$meter^3$ (kg/m^3)
Velocity	knots	0.5144	meters/second (m/sec)
	ft/sec	0.3048	
Frequency	cps	1.0	hertz (Hz)

*Multiply a value given in U.S. Customary Units by the conversion factor to obtain the equivalent value in SI Units or apply the conversion formula.

**Prefixes to indicate multiples of SI Units are as follows:

Prefix	Multiple
milli (m)	10^{-3}
kilo (k)	10^3
mega (M)	10^6
giga (G)	10^9

APPENDIX B

SPECIMENS, TEST EQUIPMENT, AND EXPERIMENTAL PROCEDURE

Specimens

The configurations of test specimens are given in figure 1. The longitudinal axis of all specimens was parallel to the rolling direction of the sheet. Specimen surfaces were left as rolled. The notch in the fatigue specimen has a theoretical elastic-stress concentration factor K_T of 4. The notch configuration simulates an ellipse as shown in the figure. The stress concentration was determined by the procedure developed by McEvily, Illg, and Hardrath (ref. 13). The radius at each end of the notch was generated by three drilling operations beginning with an 0.110-inch-diameter (2.79-mm) drill and successively increasing the diameter by increments of 0.003 inch (0.076 mm). The small burrs produced by the drilling operation were removed by holding the specimen lightly against a rotating rubber rod that was impregnated with an abrasive. The deburring operation resulted in a slight bevel around the ends of the notch.

Tensile Tests

Tensile tests were conducted in a universal hydraulic testing machine which has a 120 000-lbf (530-kN) capacity. Stress-strain curves were obtained autographically by means of an x-y plotter. The electronic signal from a load cell in series with the specimen actuated the recorder drive for the stress axis. The strain axis was actuated by the output of an extensometer that incorporated a linear variable differential transformer. The extensometer was attached to the specimen in the reduced section and had a gage length of 1.00 inch (25.4 mm). The elongation in 2.00 inches (50.8 mm) was determined by measuring the distance, after fracture, between grid lines placed on each specimen prior to the test.

Variable-Amplitude Fatigue Tests

All specimens were loaded axially in variable-amplitude fatigue tests, and test stresses were based on the initial net area of each specimen at its minimum section. The programable hydraulically actuated machines used for these tests are described in reference 2. The average operating speed for these tests was about 7 cps (7 Hz).

Specimens for elevated-temperature variable-amplitude tests were heated by the apparatus shown schematically in figure 9. The temperature was sensed by a thermocouple attached to the specimen and was controlled to within 10° F (5.5° K) of the desired temperature by a commercially available temperature controller. The guide leaves shown in the figure prevented specimens from buckling when compressive loads were applied.

Constant-Amplitude Fatigue Tests

Loads for all constant-amplitude fatigue tests were applied axially, and test stresses were based on the initial net area of each specimen at its minimum section. Two types of testing machines were used to obtain constant-amplitude fatigue data. Specimens with an expected life of more than 10 000 stress cycles were tested in machines that operated at a subresonant frequency of 30 cps (30 Hz) and are described in reference 14. Specimens with an expected life of less than 10 000 cycles were tested in a hydraulically actuated testing machine that operated at about 15 cps (15 Hz) and is described in reference 15.

For room-temperature tests, aluminum plates prevented specimens from buckling. The plates were fastened together by a row of bolts along each of the two longitudinal edges. Shims of the proper thickness between the plates and along the row of bolts prevented the guide plate from binding the specimen.

Constant-amplitude fatigue tests at 550° F (560° K) were conducted by using a heat source described in reference 15. The heat was conducted to the specimen by means of carbon slabs that acted as guide plates. This heater maintained the temperature of the specimens to within 10° F (5.5° K) of the desired temperature.

APPENDIX C

DERIVATION OF STRESS SPECTRUM AND TEST PROGRAMS

Stress Spectrum

The spectrum of wing stresses for this investigation was developed from four sources of stress: gusts, maneuvers, taxiing, and ground-air-ground cycles.

Stresses due to gusts.- Stresses due to gusts were developed on the basis of the flight profile shown in figure 10. A relation from reference 16 was used to correlate gust velocity U_{de} with a stress ratio θ. The relation in modified form for the U.S. Customary Units given in the symbol list is

$$U_{de} = \frac{498\left(m_d/A\right)g\theta}{K_g V_e a} \tag{C1}$$

where

$$K_g = \frac{0.88\mu_g}{5.3 + \mu_g}$$

and

$$\mu_g = \frac{2(m/A)}{\bar{c}a\rho}$$

Wing loading m_d/A was 2.8 slugs/ft^2 (440 kg/m^2) at maximum take-off mass, and mean geometric chord $\bar{c}$ was 40 feet (12 meters). Stress was assumed to be proportional to lift. (Because eq. (C1) was derived empirically, the constant 498 requires appropriate units.)

A mathematical expression describing the distribution of θ in the atmosphere was obtained by combining equation (C1) with an expression from reference 17 for the distribution of derived gust velocites. The resultant expression is

$$\text{Exceedances of } \theta \text{ per mile} = \underbrace{20P_1 \exp\left(\frac{-\theta F}{2.2k_1}\right)}_{\text{nonstorm}} + \underbrace{15P_2 \exp\left(\frac{-\theta F}{5.3k_2}\right)}_{\text{storm}} \tag{C2}$$

where

$$F = \frac{498\left(m_d/A\right)g}{K_g V_e a}$$

and P_1, P_2, k_1, and k_2 are turbulence factors taken from reference 17. Equation (C2) gives the total number of peaks (positive and negative) per mile (per

1600 meters) at each level of θ; to obtain the number of cycles, the number of peaks must be divided by 2.

The calculated distributions of θ for climb, cruise, and descent are shown in figure 11. The values of θ shown in the figure are 20 percent greater than the values used to calculate the exceedances; the additional stress is due to the inertia of the wing.

Stresses due to operational maneuvers.- Operational maneuvers for the subject airplane were assumed to be similar to those for current subsonic jet transports. Vertical-acceleration data from reference 18 were converted into stress terms by the following relation:

$$\theta = m^* a_n \tag{C3}$$

where m^* was assumed to be 1.00, 0.75, and 0.60 for climb, cruise, and descent, respectively. The maneuver stress data are presented in figure 12.

Stresses due to check-flight maneuvers.- Maneuvers during check flights are characteristically severe, because the purpose of check flights is to verify pilot proficiency for all expected flying conditions. In comparison with maneuvers, gusts occur very infrequently during check flights; therefore, their effects were not considered in these flights. The check-flight vertical-acceleration distribution was taken from reference 18 and converted into a distribution of θ. These data are shown in figure 13 in which distributions of positive and negative maneuvers are shown separately. (A positive maneuver creates tension in the lower wing skin, and a negative maneuver creates compression in the lower wing skin.) Check flights, in which m^* was assumed to be 0.70, made up 4 percent of the total number of flights. In each $2\frac{1}{2}$-hour check flight, seven touch-and-go landings were made.

Stresses due to taxiing.- Taxi stresses were applied according to the spectrum shown in figure 14. Although this spectrum was compiled rather arbitrarily, it is in reasonable agreement with the taxi spectrum presented in reference 12 for a four-engine turbojet airplane.

Stresses due to GAG cycles.- The GAG cycle is defined to be the variation of stress that occurs at a point in the tension surface of a wing due to the take-off and landing of an airplane. The minimum value of the GAG stress cycle depends on the details of construction of an airplane – particularly the location of the landing gear. In the present investigation, the landing gear location was assumed to be near the fuselage. A minimum stress for the GAG cycle of $-0.5S_{1g,d}$ was chosen as a representative value for most of the tests of the present investigation. In order to assess the influence of the minimum stress on fatigue life, other tests were conducted with minimum stresses of zero and $-S_{1g,d}$.

Test Stress Programs

The cumulative probabilities of occurrence of gusts and operational-maneuver stresses shown in figures 11 and 12 were combined and used as the basis for forming operational flights. The cumulative probabilities of occurrence of check-flight maneuver stresses shown in figure 13 were used as the basis for forming check flights. To extract a test stress program from the probability of occurrence, the ordinate was divided into bands. The bandwidth was selected equal to 0.1 beginning at $\theta = 0.1$. The fatigue damage due to all the stress levels within a band was assumed to be producible by one representative stress level within the band. By assuming a linear cumulative-damage rule, the representative level of a band was found in reference 1 for aluminum alloy to occur at approximately 0.4 of the bandwidth measured from the lower bound. Since the S-N curves for titanium alloys are similar in shape to those for aluminum alloys, the same representative level was used herein; thus, each test level occurred at $\theta = 0.14$, 0.24, 0.34, and so forth.

Formulation of operational flights.- Representative levels of θ that occurred at least once in each operational flight composed the basic operational flight. Representative levels of θ that occurred less than once per flight were added to the basic flight to form fifth, 100th, 1000th, and 10 000th operational flights. Thus, each fifth operational flight contained all the stresses in the basic operational flight plus those that occur once in five flights on the average; each 100th operational flight contained all the stresses in a fifth operational flight plus those that occur once in 100 flights on the average; and so forth. The stress sequence for basic operational flights is shown in figure 2(a). The number and severity of flight stresses increased from the basic flight to the 10 000th flight as shown by comparing figures 2(a) and 2(b). In tests, the simulated flights were applied in ascending order of severity; that is, four basic operational flights were applied, a fifth operational flight was applied, four more basic flights, a fifth operational flight, and so forth. The 100th, 1000th, and 10 000th flights superseded the fifth flights at the indicated times. The number of occurrences of each level of representative stress for each severity of flight is given in table VIII, and the total number of occurrences of each level of representative stress for 10 000 operational flights is given in table IX. Taxi stresses for type B tests were applied according to the numbers in table X.

Formulation of check flights.- Check flights were formed in a manner similar to that used for operational flights but were based on the stress spectrum in figure 13. The sequence in which the stresses were applied is shown in figure 2(c), and the number of occurrences of each representative stress in each check flight is given in table XI. In tests, a check flight was applied after every 24 operational flights. The 10th or 100th check flights superseded basic check flights at indicated times in a manner similar to the application of 10th and 100th operational flights. The total number of occurrences of each level of representative stress for 100 check flights is given in table XII.

REFERENCES

1. Naumann, Eugene C.; Hardrath, Herbert F.; and Guthrie, David E.: Axial-Load Fatigue Tests of 2024-T3 and 7075-T6 Aluminum-Alloy Sheet Specimens Under Constant- and Variable-Amplitude Loads. NASA TN D-212, 1959.

2. Naumann, Eugene C.: Evaluation of the Influence of Load Randomization and of Ground-Air-Ground Cycles on Fatigue Life. NASA TN D-1584, 1964.

3. Comm. on Metric Pract.: ASTM Metric Practice Guide. NBS Handbook 102, U.S. Dep. Com., Mar. 10, 1967.

4. Spaulding, E. H.: Design for Fatigue. SAE Trans., vol. 62, 1954, pp. 104-116.

5. Figge, I. E.: Residual Strength of Alloys Potentially Useful in Supersonic Aircraft. NASA TN D-2613, 1965.

6. Illg, Walter; and Castle, Claude B.: Axial-Load Fatigue Properties of PH 15-7 Mo Stainless Steel in Condition TH 1050 at Ambient Temperature and 500° F. NASA TN D-2358, 1964.

7. Trapp, W. J.: Elevated Temperature Fatigue Properties of SAE 4340 Steel. WADC Tech. Rept. 52-325, Pt. 1, U.S. Air Force, Dec. 1952.

8. Hudson, C. Michael: Studies of Fatigue Crack Growth in Alloys Suitable for Elevated-Temperature Applications. NASA TN D-2743, 1965.

9. Miner, Milton A.: Cumulative Damage in Fatigue. J. Appl. Mech., vol. 12, no. 3, Sept. 1945, pp. A-159 – A-164.

10. Hunter, Paul A.: Initial VGH Data on Operations of Small Turbojets in Commercial Transport Service. J. Aircraft, vol. 4, no. 6, Nov.-Dec. 1967, pp. 513-517.

11. Hunter, Paul A.: An Analysis of VGH Data From One Type of Four-Engine Turbojet Transport Airplane During Commercial Operations. NASA TN D-4330, 1968.

12. Coleman, Thomas L.: Trends in Repeated Loads on Transport Airplanes. NASA paper presented at the Symposium on Fatigue Design Procedures (Munich, Germany), June 16-18, 1965.

13. McEvily, Arthur J., Jr.; Illg, Walter; and Hardrath, Herbert F.: Static Strength of Aluminum-Alloy Specimens Containing Fatigue Cracks. NACA TN 3816, 1956.

14. Grover, H. J.; Hyler, W. S.; Kuhn, Paul; Landers, Charles B.; and Howell, F. M.: Axial-Load Fatigue Properties of 24S-T and 75S-T Aluminum Alloy as Determined in Several Laboratories. NACA Rept. 1190, 1954. (Supersedes NACA TN 2928.)

15. Imig, L. A.: Effect of Initial Loads and of Moderately Elevated Temperature on the Room-Temperature Fatigue Life of Ti-8Al-1Mo-1V Titanium-Alloy Sheet. NASA TN D-4061, 1967.

16. Anon.: Airplane Airworthiness; Transport Categories. Civil Aero. Manual 4b, Federal Aviation Agency, May 1, 1960.

17. Press, Harry; and Steiner, Roy: An Approach to the Problem of Estimating Severe and Repeated Gust Loads for Missile Operations. NACA TN 4332, 1958.

18. Staff of Langley Airworthiness Branch: Operational Experiences of Turbine-Powered Commercial Transport Airplanes. NASA TN D-1392, 1962.

TABLE I.- CHEMICAL COMPOSITION OF DUPLEX-ANNEALED Ti-8Al-1Mo-1V TITANIUM-ALLOY SHEET

[Information supplied by manufacturer]

Mill heat	Weight percentage of constituent							
	C	Fe	N	Al	V	Mo	H	Ti
I	0.026	0.11	0.011	7.9	1.0	1.1	0.003 to 0.006	Balance
II	.025	.07	.010	7.8	1.0	1.1	.008 to .009	Balance
III	.025	.05	.012	7.8	1.0	1.1	.010 to .011	Balance

TABLE II.- LONGITUDINAL TENSILE PROPERTIES OF DUPLEX-ANNEALED[a] Ti-8Al-1Mo-1V TITANIUM-ALLOY SHEET 0.050 INCH (1.27 mm) THICK

Mill heat	Sheet	Ultimate tensile strength		Tensile yield strength at 0.2% offset		Young's modulus		Elongation in 2 in. (50.8 mm), percent
		ksi	MN/m^2	ksi	MN/m^2	ksi	GN/m^2	
Properties at room temperature (values are averages of 16 tests)								
I	24	[b]150.2	[b]1036	[b]135.0	[b]931	[b]17 400	[b]120	[b]12.0
	29	144.9	999	132.1	911	16 700	115	13.0
	30	150.4	1037	136.9	944	17 200	119	12.5
	34	151.0	1041	136.9	944	16 900	116	12.7
	35	149.1	1028	135.3	933	16 600	114	12.3
II	36	145.3	1002	133.7	922	17 400	120	12.1
	37	142.1	980	130.0	896	17 200	119	12.2
	40	144.2	994	131.2	905	17 200	119	12.5
	41	145.1	1000	133.0	917	17 200	119	12.3
III	46	145.5	1003	133.1	918	17 300	119	14.6
Properties at 550° F (560° K) (values are averages of three tests)								
I	24	118.3	816	98.5	679	16 000	110	11.2

[a]Duplex-annealing procedure consisted of heating to 1450° F (1060° K) for 8 hours, furnace cooling, heating to 1450° F (1060° K) for 15 minutes, and air cooling.

[b]Average of three tests.

TABLE III.- VARIABLE-AMPLITUDE FATIGUE LIVES AT ROOM TEMPERATURE FOR NOTCHED ($K_T = 4$) SPECIMENS OF DUPLEX-ANNEALED Ti-8Al-1Mo-1V TITANIUM-ALLOY SHEET 0.050 INCH (1.27 mm) THICK

[Minimum stress for ground-air-ground cycle was $-0.5S_{1g,d}$ unless otherwise noted]

Test type	$S_{1g,d}$		Stress at failure (a)			Fatigue life, flights	
	ksi	MN/m^2	θ	Segment of flight	Kind of flight	Individual	Geometric mean
A	25	170	---	------	-----	>52 000	>52 000
			---	------	-----	>52 000	
			---	------	-----	>52 000	
			---	------	-----	>52 000	
	30	210	0.24	Climb	5th	13 400	16 600
			.24	Climb	Basic	33 300	
			.24	Climb	Basic	16 600	
			.64	Climb	100th	14 800	
			.44	Climb	5th	13 900	
			---	------	-----	17 560	
			---	------	-----	12 774	
	35	240	0.44	Climb	5th	7 850	7 150
			---	Climb	1000th	7 270	
			.44	Climb	5th	6 420	
			.44	Climb	5th	7 520	
			---	Climb	5th	7 950	
			.84	Climb	1000th	8 300	
			.44	Climb	5th	6 540	
			---	------	-----	7 070	
			.44	Climb	5th	5 800	
B	25	170	---	------	-----	>52 000	41 500
			0.24	Climb	Basic	37 200	
			.44	Climb	5th	46 600	
	30	210	0.44	Climb	5th	16 100	14 800
			.44	Climb	5th	15 000	
			.44	Climb	5th	13 500	
	35	240	0.64	Climb	100th	7 800	7 000
			.44	Climb	5th	6 600	
			.34	Climb	5th	6 700	

[a]All specimens failed during operational flights.

TABLE III.- VARIABLE-AMPLITUDE FATIGUE LIVES AT ROOM TEMPERATURE FOR NOTCHED ($K_T = 4$) SPECIMENS OF DUPLEX-ANNEALED Ti-8Al-1Mo-1V TITANIUM-ALLOY SHEET 0.050 INCH (1.27 mm) THICK – Concluded

Test type	$S_{1g,d}$		Stress at failure (a)			Fatigue life, flights	
	ksi	MN/m^2	θ	Segment of flight	Kind of flight	Individual	Geometric mean
C	25	170	0.14	Cruise	Basic	40 940	26 800
			.44	Climb	5th	26 700	
			.84	Climb	1000th	17 700	
	30	210	0.24	Cruise	100th	11 600	9 600
			---	Climb	Basic	8 950	
			.14	Cruise	Basic	8 450	
	35	240	0.14	Cruise	Basic	5 650	5 600
			---	Climb	Basic	5 150	
			.24	Cruise	5th	5 920	
D	25	170	---	------	-----	>52 000	>52 000
			---	------	-----	>52 000	
			---	------	-----	>52 000	
	30	210	0.44	Climb	5th	17 200	12 300
			---	------	-----	>52 000	
			.14	Climb	Basic	12 300	
			.14	Climb	5th	8 250	
			.44	Climb	5th	13 200	
	35	240	0.44	Climb	5th	5 250	6 200
			.54	Climb	100th	6 450	
			---	Climb	-----	7 070	
E	[b]30	[b]210	0.14	Climb	Basic	42 430	>52 000
			---	-----	-----	>52 000	
			---	-----	-----	>52 000	
			---	-----	-----	>52 000	
			---	-----	-----	>52 000	
	[c]30	[c]210	0.14	Climb	100th	7 100	8 500
			.14	Climb	1000th	7 300	
			.14	Climb	Basic	12 800	
			.14	Climb	5th	9 400	
			.14	Climb	5th	7 100	

[a]All specimens failed during operational flights.

[b]Minimum stress for ground-air-ground cycle was zero.

[c]Minimum stress for ground-air-ground cycle was $-S_{1g,d}$.

TABLE IV.- VARIABLE-AMPLITUDE FATIGUE LIVES AT 550° F (560° K) FOR NOTCHED ($K_T = 4$) SPECIMENS OF DUPLEX-ANNEALED Ti-8Al-1Mo-1V TITANIUM-ALLOY SHEET 0.050 INCH (1.27 mm) THICK

[Minimum stress for ground-air-ground cycle was $-0.5S_{1g,d}$ unless otherwise noted]

Test type	$S_{1g,d}$ ksi	$S_{1g,d}$ MN/m^2	Stress at failure (a) θ	Segment of flight	Kind of flight	Fatigue life, flights: Individual	Geometric mean
A	25	170	0.24	Climb	5th	18 160	27 300
			.34	Climb	1000th	17 680	
			---	-------	-------	>52 000	
			.14	Climb	Basic	34 040	
			.14	Climb	5th	42 700	
			.44	Climb	5th	32 500	
	30	210	0.14	Climb	5th	7 130	7 000
			.44	Climb	5th	6 900	
			.44	Climb	5th	7 554	
			.64	Climb	100th	6 448	
	35	240	0.14	Climb	5th	4 350	4 100
			.34	Climb	Basic	4 110	
			.24	Climb	5th	3 900	
B	25	170	0.44	Climb	5th	14 000	16 500
			.64	Climb	100th	16 100	
			.14	Climb	Basic	19 900	
	30	210	0.44	Climb	5th	6 150	6 500
			.14	Climb	5th	7 750	
			.44	Climb	5th	5 850	
	35	240	0.44	Climb	5th	3 680	3 300
			.54	Climb	100th	2 920	
			.14	Climb	5th	3 350	
C	25	170	0.14	Cruise	5th	19 600	19 000
			.14	Cruise	Basic	18 100	
			.14	Climb	Basic	19 200	
	30	210	0.64	Climb	100th	6 420	5 750
			.14	Cruise	100th	5 500	
			.14	Cruise	Basic	5 300	
	35	240	0.24	Cruise	5th	3 450	2 850
			.14	Cruise	Basic	2 800	
			.24	Cruise	5th	2 410	
D	25	170	---	-------	-------	>52 000	13 600
			0.44	Climb	5th	17 800	
			1.14	Climb	10 000th	10 400	
	30	210	0.14	Climb	100th	6 350	6 700
			.44	Descent	Basic	7 750	
			.84	Climb	1000th	6 240	
	35	240	0.44	Climb	5th	2 640	3 100
			.14	Climb	5th	3 260	
			.14	Climb	Basic	3 460	
E	[b]30	[b]210	0.64	Climb	100th	9 200	16 000
			.64	Climb	100th	28 000	
			---	-------	-------	>52 000	
	[c]30	[c]210	0.14	Climb	Basic	3 780	4 500
			.44	Climb	5th	4 100	
			.24	Climb	Basic	5 850	

[a]All specimens failed during operational flights.

[b]Minimum stress for ground-air-ground cycle was zero.

[c]Minimum stress for ground-air-ground cycle was $-S_{1g,d}$.

TABLE V.- CONSTANT-AMPLITUDE FATIGUE LIVES AT ROOM TEMPERATURE FOR NOTCHED (K_T = 4) SPECIMENS OF DUPLEX-ANNEALED Ti-8Al-1Mo-1V TITANIUM-ALLOY SHEET 0.050 INCH (1.27 mm) THICK

Maximum stress, ksi	Maximum stress, MN/m^2	Fatigue life, cycles	Geometric mean fatigue life, cycles
S_{mean} = -15 ksi (-103 MN/m^2)			
45	310	3 320	3 380
		3 400	
		3 430	
35	241	9 020	9 330
		9 410	
		9 560	
25	172	28 000	29 500
		28 000	
		33 000	
15	103	171 000	215 000
		237 000	
		248 000	
13	90	425 000	616 000
		581 000	
		942 000	
12	83	448 000	656 000
		703 000	
		896 000	
11	76	1 302 000	3 142 000
		7 583 000	
		>10 000 000	
10	69	>10 000 000	>10 000 000
S_{mean} = 0			
60	414	1 510	1 730
		1 730	
		2 000	
50	345	4 330	4 400
		4 400	
		4 560	
40	276	13 000	13 400
		13 020	
		13 340	
		14 430	
30	207	36 000	51 000
		50 000	
		54 000	
		54 000	
		65 000	
25	172	147 000	286 000
		175 000	
		243 000	
		451 000	
		681 000	
20	138	2 956 000	6 450 000
		3 882 000	
		7 588 000	
		7 808 000	
		>10 000 000	

TABLE V.- CONSTANT-AMPLITUDE FATIGUE LIVES AT ROOM TEMPERATURE FOR NOTCHED ($K_T = 4$) SPECIMENS OF DUPLEX-ANNEALED Ti-8Al-1Mo-1V TITANIUM-ALLOY SHEET 0.050 INCH (1.27 mm) THICK – Concluded

Maximum stress		Fatigue life, cycles	Geometric mean fatigue life, cycles
ksi	MN/m^2		
S_{mean} = 25 ksi (172 MN/m^2)			
80	552	1 360	1 365
		1 370	
70	483	3 340	3 515
		3 700	
60	414	9 690	9 720
		9 750	
55	379	15 000	17 550
		18 000	
		20 000	
50	345	24 320	30 410
		28 000	
		28 820	
		30 000	
		34 430	
		39 000	
44	303	33 000	44 000
		48 000	
		54 000	
40	276	61 000	306 100
		185 000	
		2 541 000	
36	248	136 000	528 000
		205 000	
		5 284 000	
34	234	400 000	400 000
		>10 000 000	
S_{mean} = 50 ksi (345 MN/m^2)			
80	552	5 230	6 250
		6 660	
		7 020	
75	517	10 580	11 500
		11 070	
		12 970	
65	448	37 000	48 700
		53 000	
		59 000	
60	414	122 000	304 600
		186 000	
		1 246 000	
58	400	1 916 000	3 622 000
		2 446 000	
		10 140 000	
56	386	>10 000 000	>10 000 000

TABLE VI.- CONSTANT-AMPLITUDE FATIGUE LIVES AT 550° F (560° K) FOR NOTCHED (K_T = 4) SPECIMENS OF DUPLEX-ANNEALED Ti-8Al-1Mo-1V TITANIUM-ALLOY SHEET 0.050 INCH (1.27 mm) THICK

Maximum stress		Fatigue life, cycles	Geometric mean fatigue life, cycles
ksi	MN/m^2		
S_{mean} = -15 ksi (-103 MN/m^2)			
40	276	3 230	3 367
		3 510	
30	207	11 040	15 000
		12 100	
		25 640	
20	138	42 000	45 000
		46 000	
		47 000	
10	69	573 000	1 045 000
		587 000	
		3 392 000	
S_{mean} = 0			
50	345	2 870	2 950
		2 900	
		3 080	
40	276	10 010	17 800
		19 490	
		28 930	
30	207	29 000	30 000
		29 000	
		31 000	
25	172	77 000	236 000
		215 000	
		795 000	
20	138	1 153 000	1 960 000
		2 363 000	
		2 800 000	
18	124	4 430 000	7 750 000
		10 256 000	
		10 318 000	
S_{mean} = 25 ksi (172 MN/m^2)			
75	517	1 340	1 390
		1 360	
		1 480	
70	482	2 430	2 560
		2 450	
		2 510	
		2 630	
		2 730	

TABLE VI.- CONSTANT-AMPLITUDE FATIGUE LIVES AT 550° F (560° K) FOR NOTCHED ($K_T = 4$) SPECIMENS OF DUPLEX-ANNEALED Ti-8Al-1Mo-1V TITANIUM-ALLOY SHEET 0.050 INCH (1.27 mm) THICK – Concluded

Maximum stress		Fatigue life, cycles	Geometric mean fatigue life, cycles
ksi	MN/m^2		
S_{mean} = 25 ksi (172 MN/m^2)			
65	448	3 690	4 030
		3 900	
		4 140	
		4 180	
		4 290	
60	414	6 860	7 250
		7 050	
		7 150	
		7 420	
		7 690	
55	379	8 000	10 700
		11 270	
		11 510	
		12 740	
50	345	18 000	21 000
		18 000	
		18 000	
		20 620	
		22 180	
		24 750	
		27 000	
45	310	36 000	212 000
		312 000	
		316 000	
		577 000	
40	276	62 000	743 000
		979 000	
		2 012 000	
		2 513 000	
38	262	1 798 000	3 760 000
		7 873 000	
36	248	>10 000 000	>10 000 000
S_{mean} = 50 ksi (345 MN/m^2)			
75	517	7 000	8 000
		8 000	
		9 000	
65	448	53 000	118 000
		60 000	
		522 000	
60	414	2 784 000	2 890 000
		2 912 000	
		2 977 000	
58	400	>10 000 000	>10 000 000

TABLE VII.- SUMMARY OF CUMULATIVE-DAMAGE ANALYSIS

[Specimens were notched ($K_T = 4$) duplex-annealed Ti-8Al-1Mo-1V titanium-alloy sheet 0.050 inch (1.27 mm) thick]

Test type	Operational flights						Check flights						Total		
	Gusts and maneuvers			GAG cycles (a)			Maneuvers			GAG cycles (b)					
	$S_{1g,d}$, ksi (MN/m^2)			$S_{1g,d}$, ksi (MN/m^2)			$S_{1g,d}$, ksi (MN/m^2)			$S_{1g,d}$, ksi (MN/m^2)			$S_{1g,d}$, ksi (MN/m^2)		
	25 (170)	30 (210)	35 (240)	25 (170)	30 (210)	35 (240)	25 (170)	30 (210)	35 (240)	25 (170)	30 (210)	35 (240)	25 (170)	30 (210)	35 (240)
$\sum \frac{n}{N}$ at failure for tests at room temperature															
A	[c]0.053	0.085	0.156	[c]0.601	0.535	0.451	[c]0.001	0.003	0.007	[c]0.028	0.054	0.062	[c]0.683	0.677	0.676
B	0.042	0.076	0.153	0.479	0.477	0.441	0.001	0.003	0.007	0.022	0.048	0.060	0.544	0.604	0.661
C	0.030	0.055	0.128	0.567	0.498	0.500	0.001	0.002	0.006	0.014	0.031	0.048	0.612	0.586	0.682
D	[c]0.053	0.064	0.139	[c]0.601	0.396	0.391	[c]0.001	0.002	0.006	[c]0.028	0.040	0.053	[c]0.683	0.502	0.589
E, $\theta_{min} = 0$	-----	[c]0.268	----	-----	[c,d]0.799	----	-----	[c]0.009	----	-----	[c,d]0.057	----	-----	[c]1.133	----
E, $\theta_{min} = -1$	-----	0.044	----	-----	[e]0.458	----	-----	0.002	----	-----	[f]0.051	----	-----	0.555	----
$\sum \frac{n}{N}$ at failure for tests at 550° F (560° K)															
A	0.007	0.011	0.027	0.369	0.260	0.367	0	0.001	0.001	0.021	0.022	0.029	0.397	0.294	0.424
B	0.004	0.010	0.021	0.223	0.241	0.296	0	0.001	0.001	0.013	0.021	0.023	0.240	0.273	0.341
C	0.005	0.009	0.019	0.402	0.327	0.374	0	0	0.001	0.015	0.018	0.020	0.422	0.354	0.414
D	0.004	0.010	0.020	0.184	0.249	0.278	0	0	0.001	0.010	0.021	0.022	0.198	0.280	0.321
E, $\theta_{min} = 0$	-----	0.025	----	-----	[d]0.217	----	-----	0.001	----	-----	[d]0.017	----	-----	0.260	----
E, $\theta_{min} = -1$	-----	0.007	----	-----	[e]0.333	----	-----	0	----	-----	[f]0.010	----	-----	0.350	----

[a] θ_{min} for ground-air-ground cycle was -0.5 unless otherwise noted.

[b] θ_{min} for ground-air-ground cycle was -0.35 unless otherwise noted.

[c] Specimens did not fail.

[d] θ_{min} for ground-air-ground cycle was zero.

[e] θ_{min} for ground-air-ground cycle was -1.0.

[f] θ_{min} for ground-air-ground cycle was -0.7.

TABLE VIII.- NUMBER OF STRESS CYCLES DUE TO GUSTS AND MANEUVERS FOR SIMULATED OPERATIONAL FLIGHTS OF A SUPERSONIC TRANSPORT

θ	Stress cycles for –			Total stress cycles
	Climb	Cruise	Descent	
Basic flight				
0.14	30	7	9	53
.24	6	---	---	
.34	1	---	---	
5th flight				
0.14	30	7	11	62
.24	8	1	2	
.34	2	---	---	
.44	1	---	---	
100th flight				
0.14	30	7	11	102
.24	18	6	7	
.34	2	4	4	
.44	7	---	---	
.54	5	---	---	
.64	1	---	---	
1000th flight				
0.14	30	7	11	127
.24	18	6	7	
.34	2	10	2	
.44	7	7	2	
.54	11	---	---	
.64	3	---	---	
.74	3	---	---	
.84	1	---	---	
10 000th flight				
0.14	30	7	11	164
.24	18	6	7	
.34	2	10	2	
.44	7	7	4	
.54	11	7	5	
.64	3	---	2	
.74	6	---	1	
.84	6	---	---	
.94	7	---	---	
1.04	3	---	---	
1.14	2	---	---	

TABLE IX.- TOTAL NUMBER OF STRESS CYCLES DUE TO GUSTS AND MANEUVERS FOR 10 000 SIMULATED OPERATIONAL FLIGHTS OF A SUPERSONIC TRANSPORT

θ	Stress cycles for –		
	Climb	Cruise	Descent
0.14	300 000	70 000	94 000
.24	65 000	2 500	4 500
.34	12 000	460	380
.44	2 600	70	22
.54	560	7	5
.64	120	-----	2
.74	33	-----	1
.84	15	-----	-----
.94	7	-----	-----
1.04	3	-----	-----
1.14	2	-----	-----
Totals . . .	380 340	73 037	98 910

TABLE X.- NUMBER OF STRESS CYCLES DUE TO TAXIING FOR SIMULATED OPERATIONAL FLIGHTS OF A SUPERSONIC TRANSPORT (USED ONLY FOR TEST TYPE B)

Flight	Taxi stresses for θ of –						Total taxi stresses per flight
	0.24	0.34	0.44	0.54	0.64	0.74	
Basic	1	---	---	---	---	---	1
5th	1	1	---	---	---	---	2
100th	1	3	2	---	---	---	6
1 000th	1	6	6	3	---	---	16
10 000th	1	6	6	6	4	1	24
Total in 10 000 flights . . .	10 000	2230	240	33	4	1	

TABLE XI.- NUMBER OF STRESS CYCLES DUE TO MANEUVERS FOR SIMULATED CHECK FLIGHTS OF A SUPERSONIC TRANSPORT ($m^* = 0.70$)

θ		Number of occurrences of stress cycles
Positive	Negative	
Basic flight		
0.14	0.14	91
.24	.14	23
.34	.24	6
.44	.24	2
10th flight		
0.14	0.14	91
.24	.14	23
.34	.24	2
.44	.24	2
.54	.34	6
.64	.44	1
100th flight		
0.14	0.14	91
.24	.14	23
.34	.24	2
.44	.24	2
.54	.34	6
.64	.44	6
.74	.54	3

TABLE XII.- TOTAL NUMBER OF STRESS CYCLES DUE TO MANEUVERS FOR 100 SIMULATED CHECK FLIGHTS OF A SUPERSONIC TRANSPORT ($m^* = 0.70$)

θ		Number of occurrences of stress cycles
Positive	Negative	
0.14	0.14	9 100
.24	.14	2 300
.34	.24	560
.44	.24	200
.54	.34	60
.64	.44	15
.74	.54	3
Total		12 238

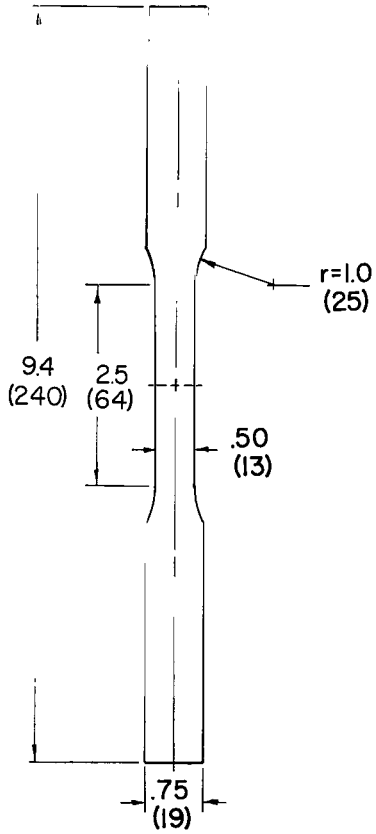

(a) Tensile specimen.

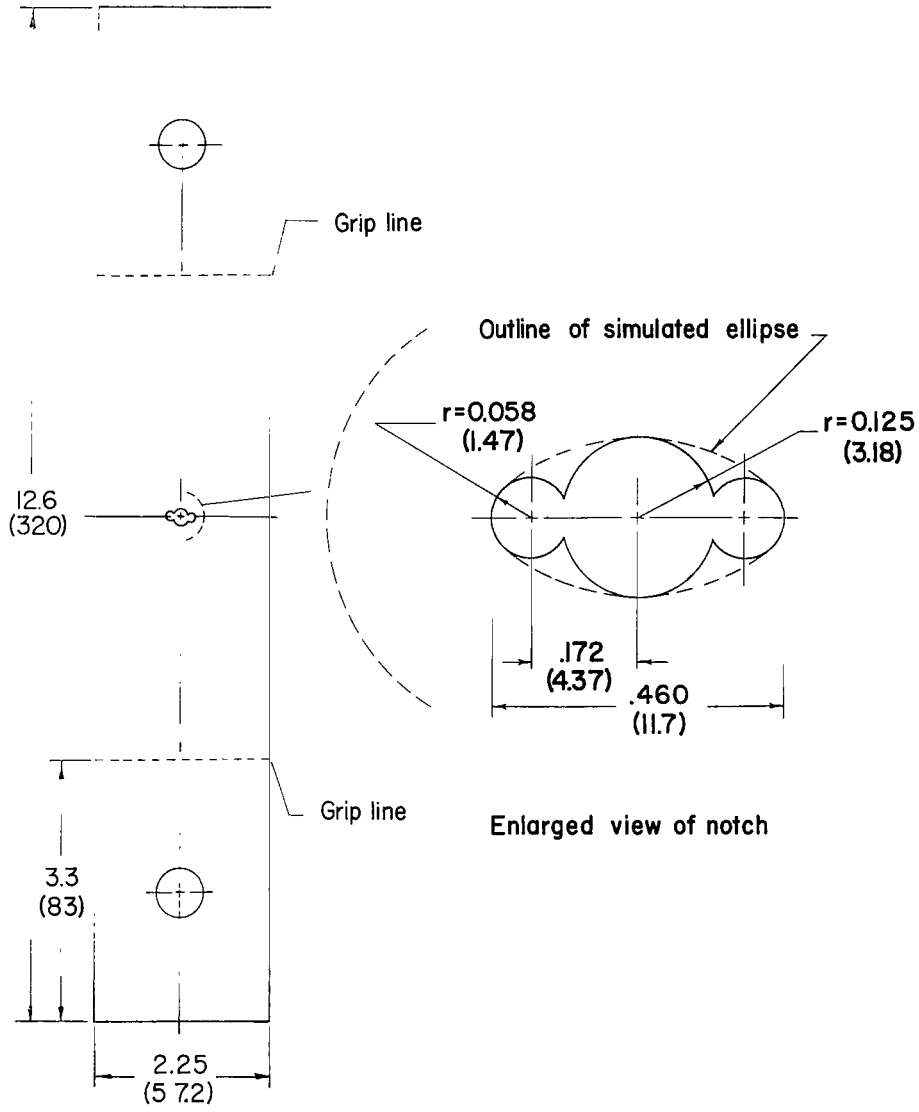

(b) Fatigue specimen.

Figure 1.- Tensile and fatigue specimen configurations. (Dimensions are in inches with millimeter equivalents in parentheses.)

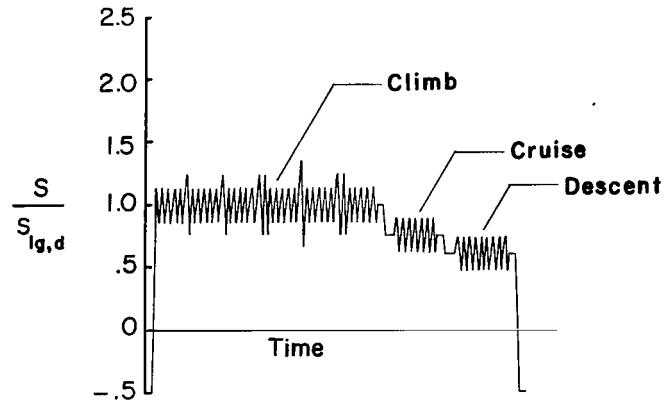

(a) Stress sequence of the basic operational flight for type A tests.

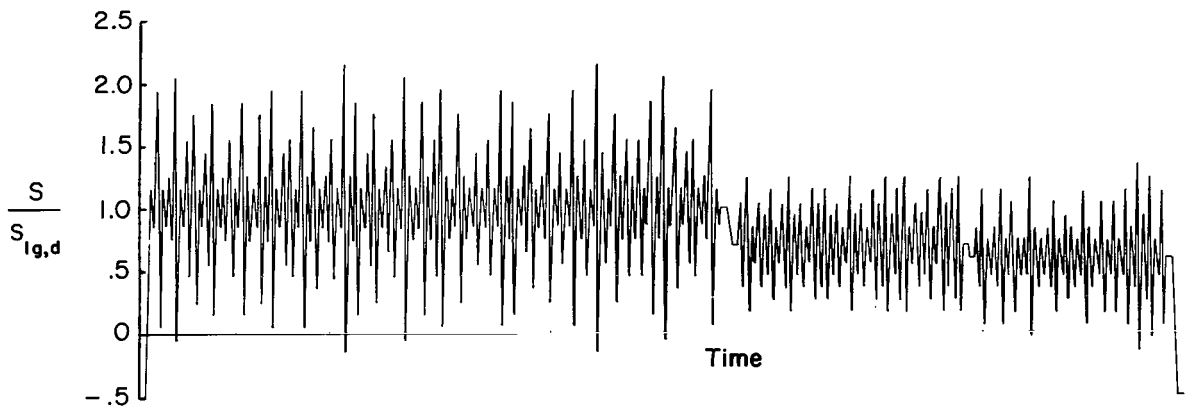

(b) Stress sequence of the 10 000th operational flight for type A tests.

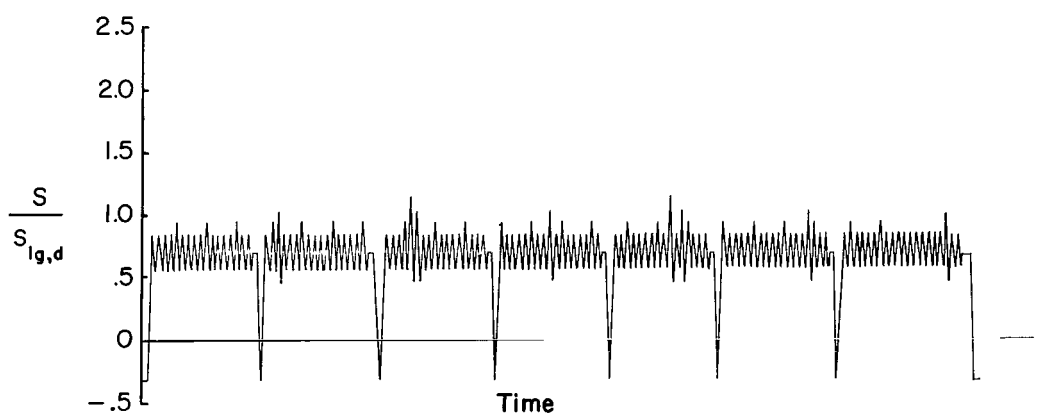

(c) Stress sequence of the basic check flight.

Figure 2.- Stress sequences for operational and check flights. (Numbers of cycles shown were applied in tests.)

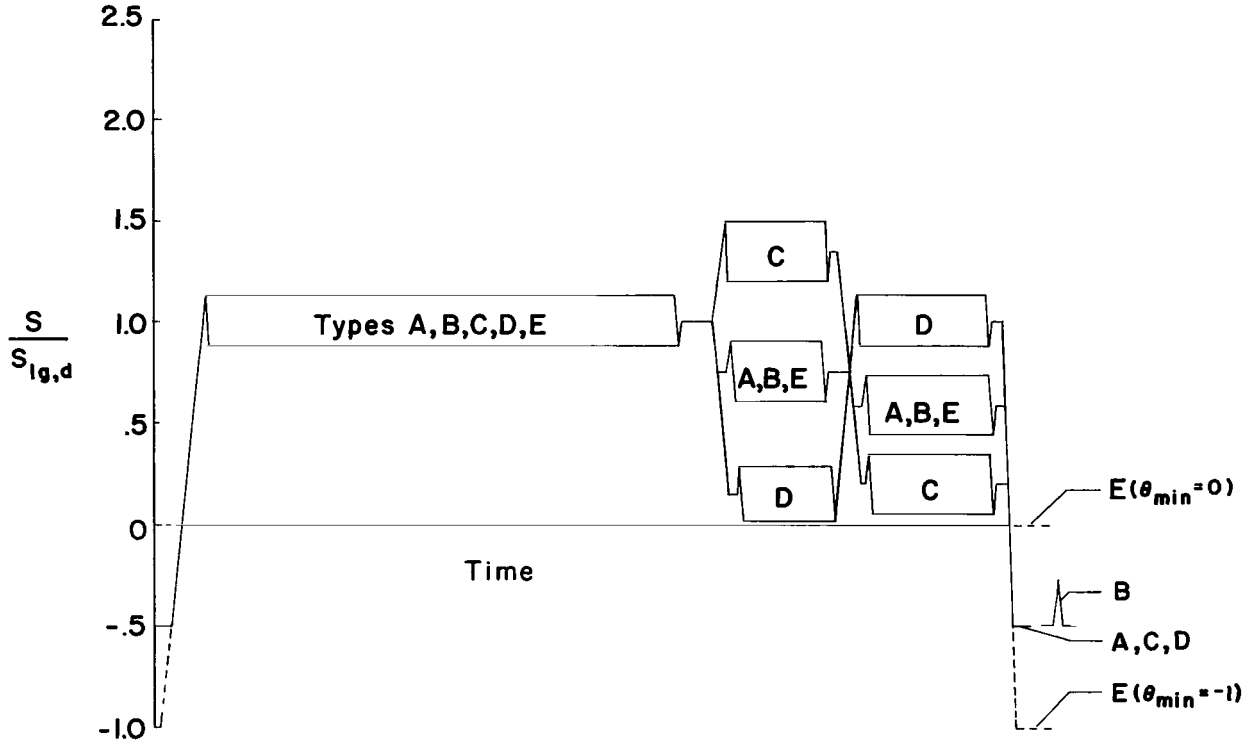

Figure 3.- Variations of stress for each type of variable-amplitude fatigue test. (See fig. 2(a).)

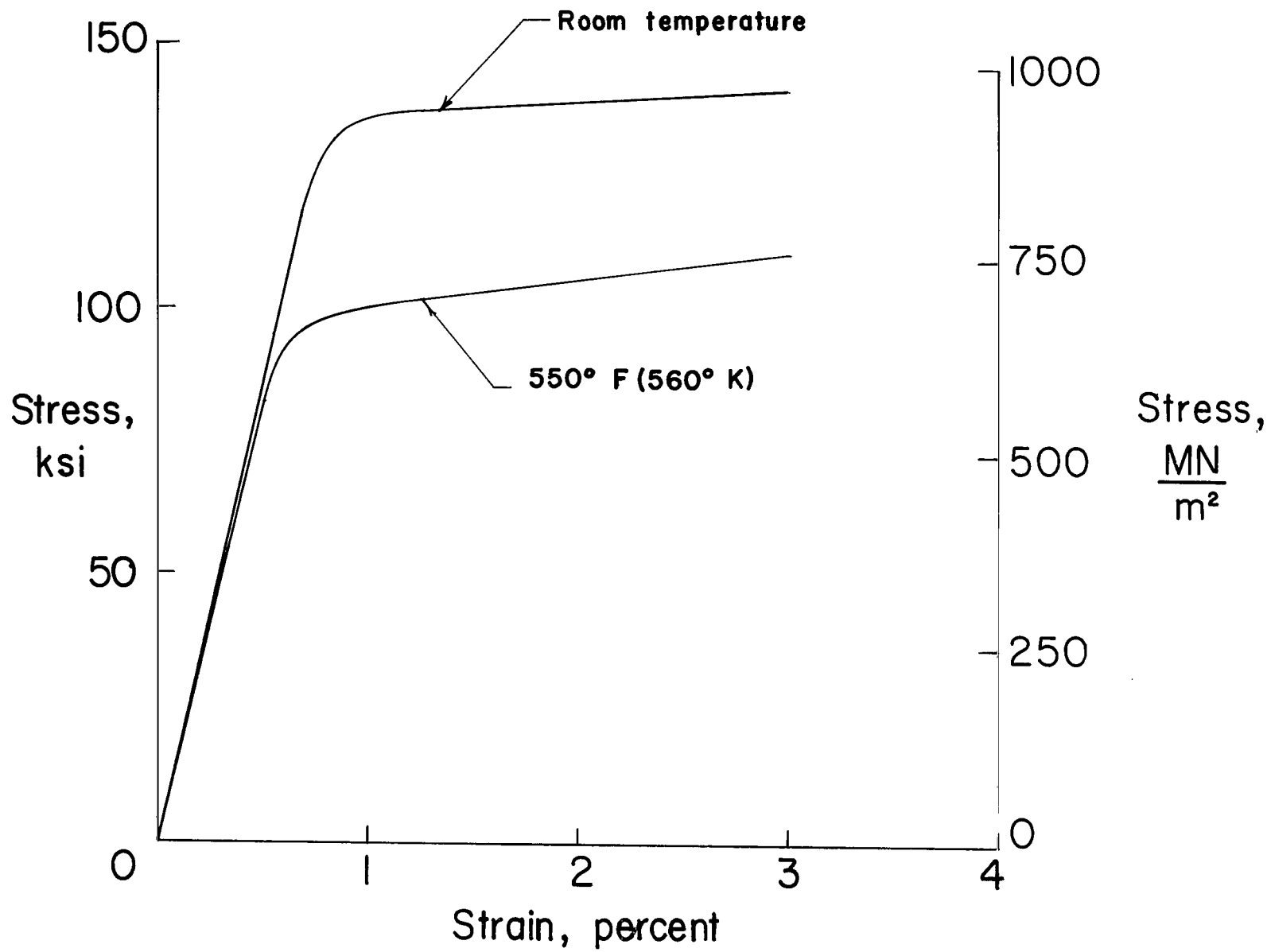

Figure 4.- Stress-strain curves at room temperature and 550° F (560° K) for duplex-annealed Ti-8Al-1Mo-1V titanium-alloy sheet. Sheet thickness was 0.050 inch (1.27 mm).

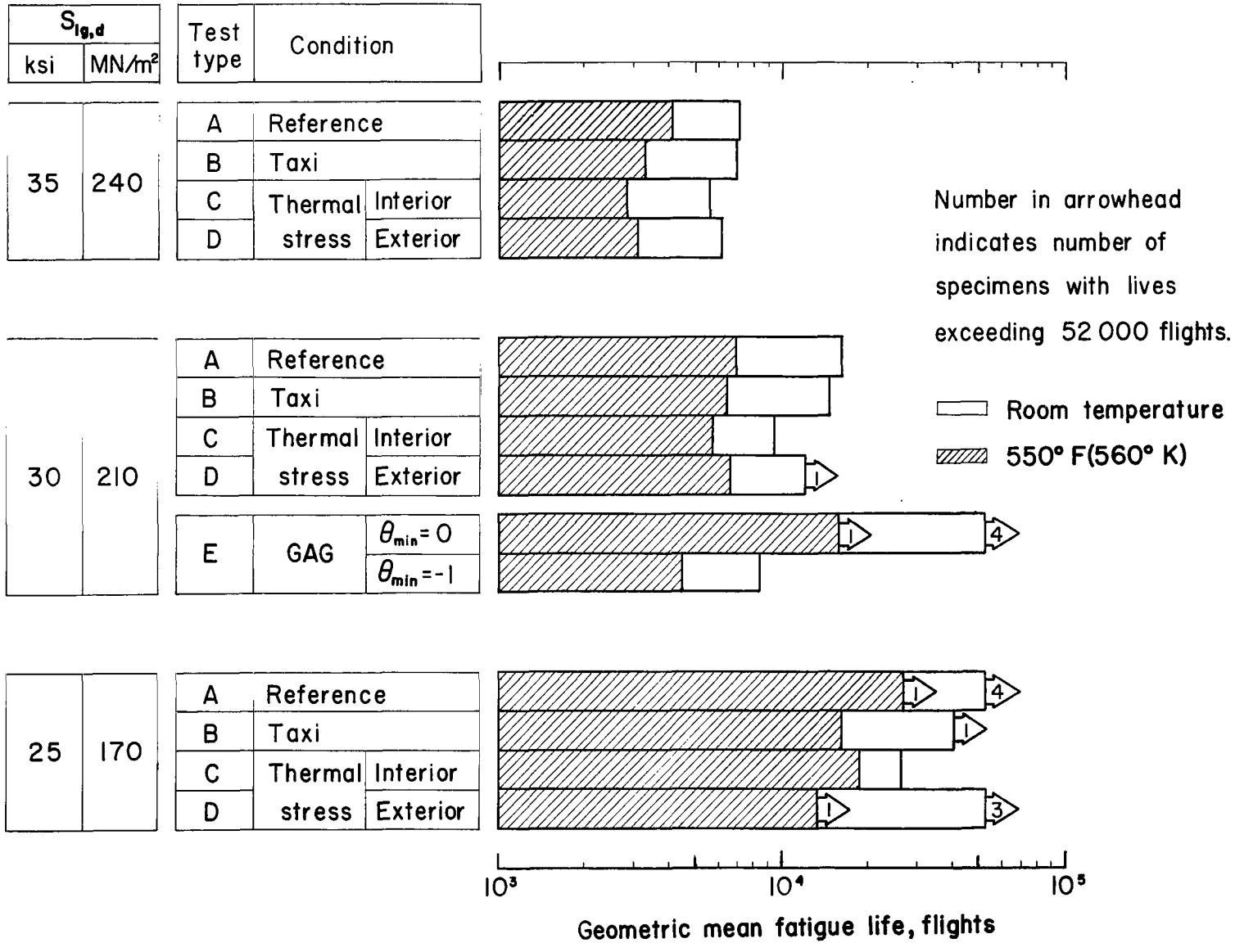

Figure 5.- Variable-amplitude fatigue lives of notched (K_T = 4) specimens of duplex-annealed Ti-8Al-1Mo-1V titanium-alloy sheet at room temperature and 550° F (560° K). Sheet thickness was 0.050 inch (1.27 mm).

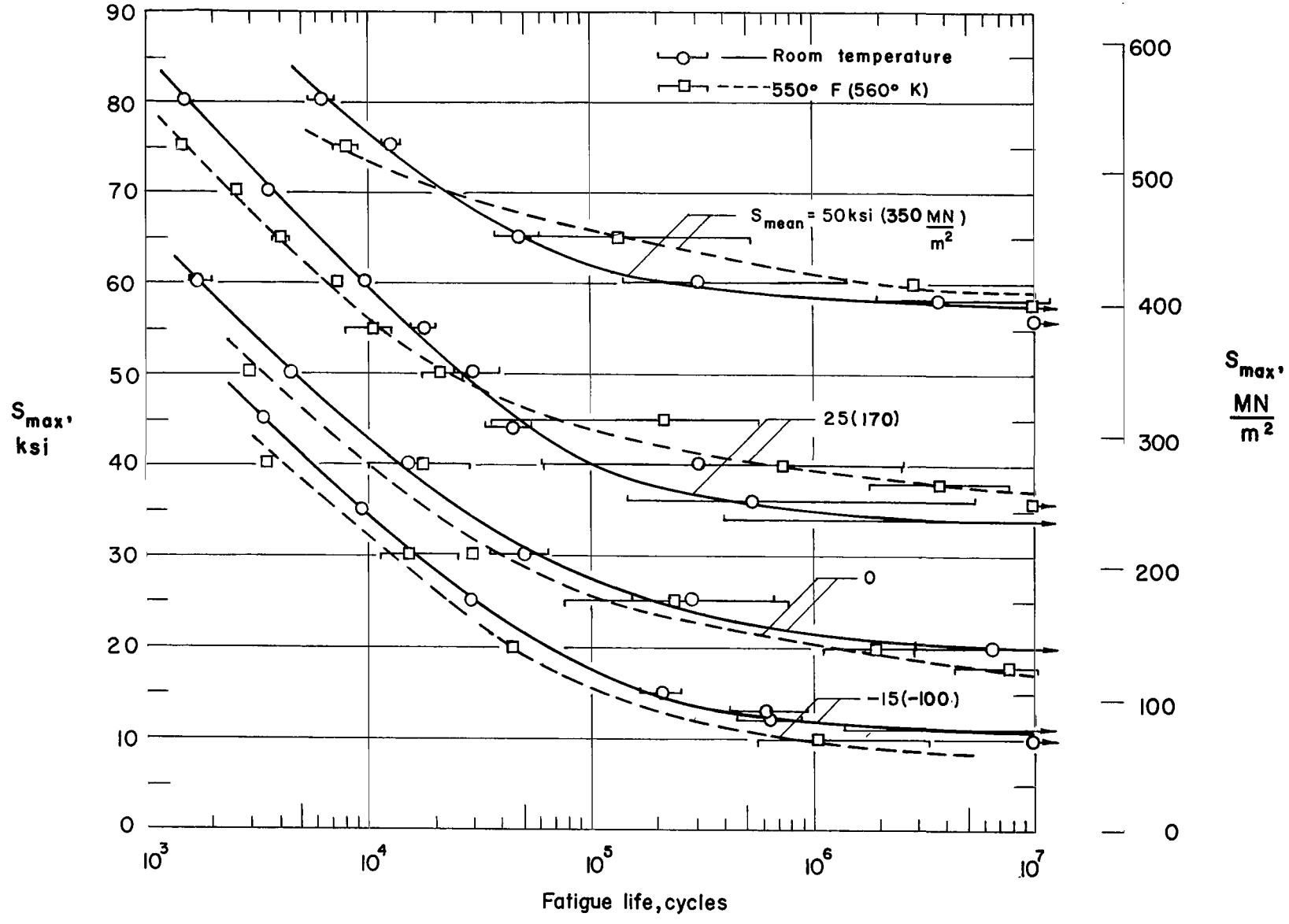

Figure 6.- Maximum stress as a function of fatigue life for constant-amplitude fatigue tests on notched (K_T = 4) specimens of duplex-annealed Ti-8Al-1Mo-1V titanium-alloy sheet at room temperature and 550° F (560° K). Sheet thickness was 0.050 inch (1.27 mm).

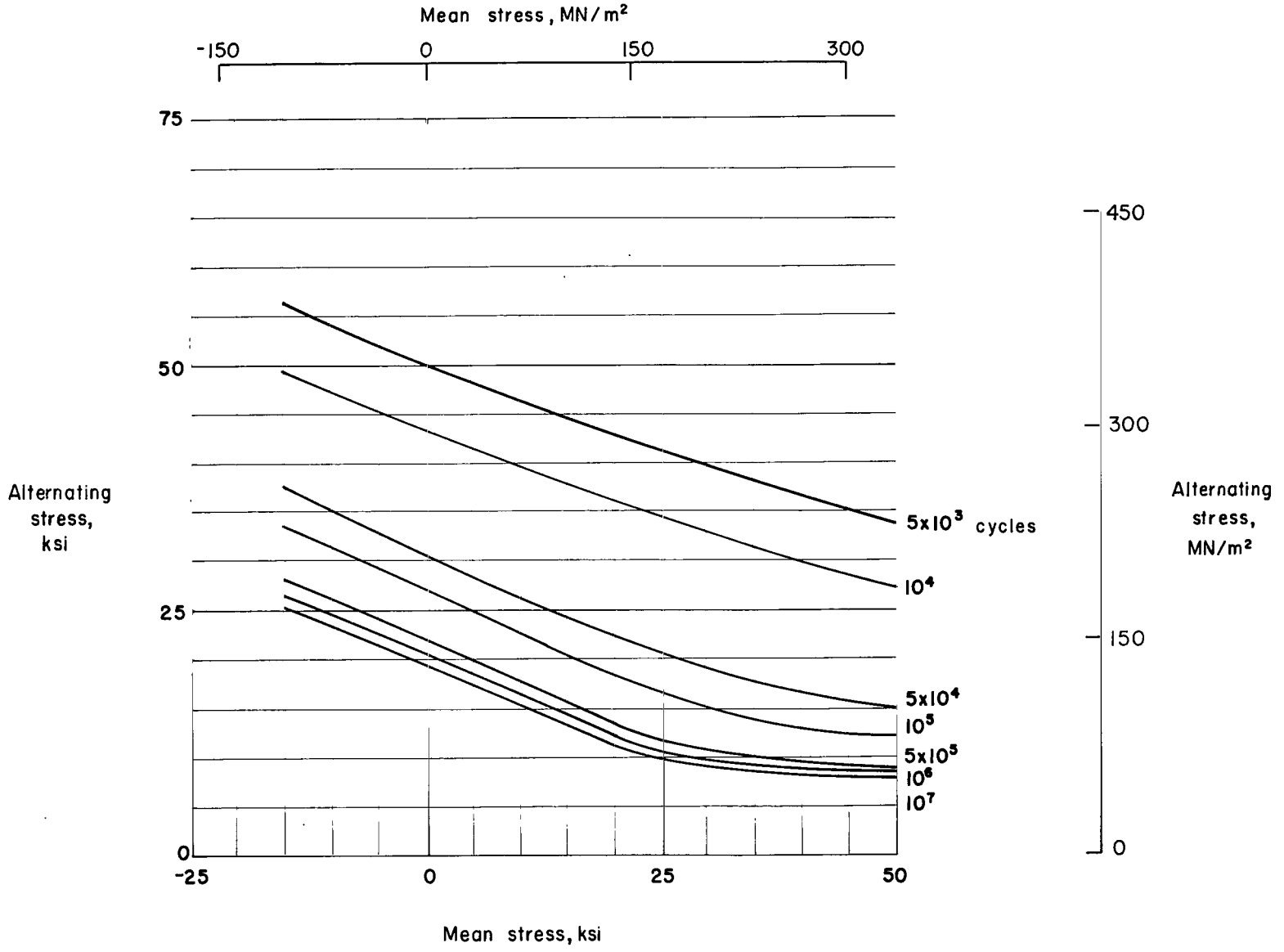

Figure 7.- Alternating stress as a function of mean stress for constant-amplitude fatigue tests on notched ($K_T = 4$) specimens of duplex-annealed Ti-8Al-1Mo-1V titanium-alloy sheet at room temperature. Sheet thickness was 0.050 inch (1.27 mm).

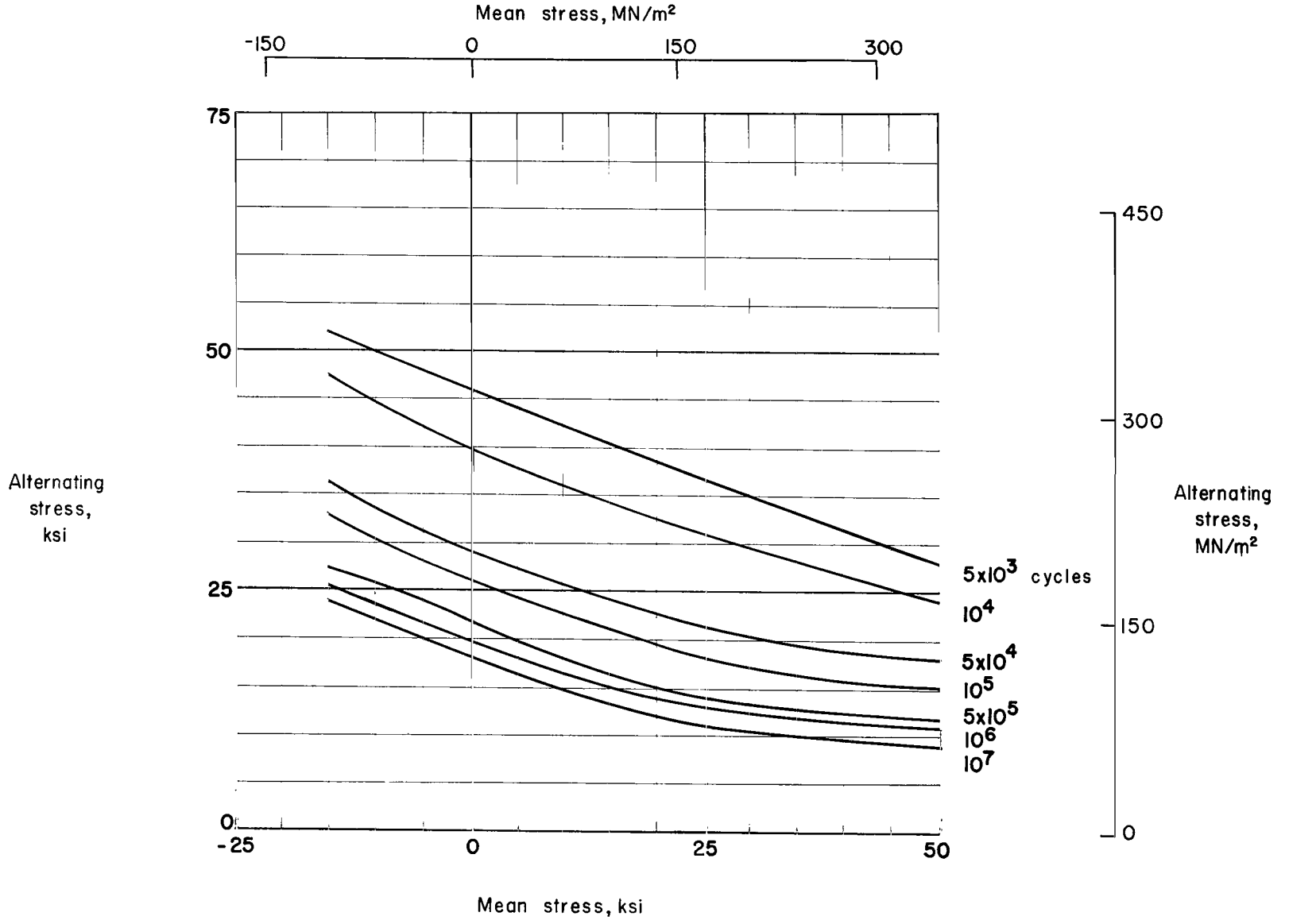

Figure 8.- Alternating stress as a function of mean stress for constant-amplitude fatigue tests on notched ($K_T = 4$) specimens of duplex-annealed Ti-8Al-1Mo-1V titanium-alloy sheet at 550° F (560° K). Sheet thickness was 0.050 inch (1.27 mm).

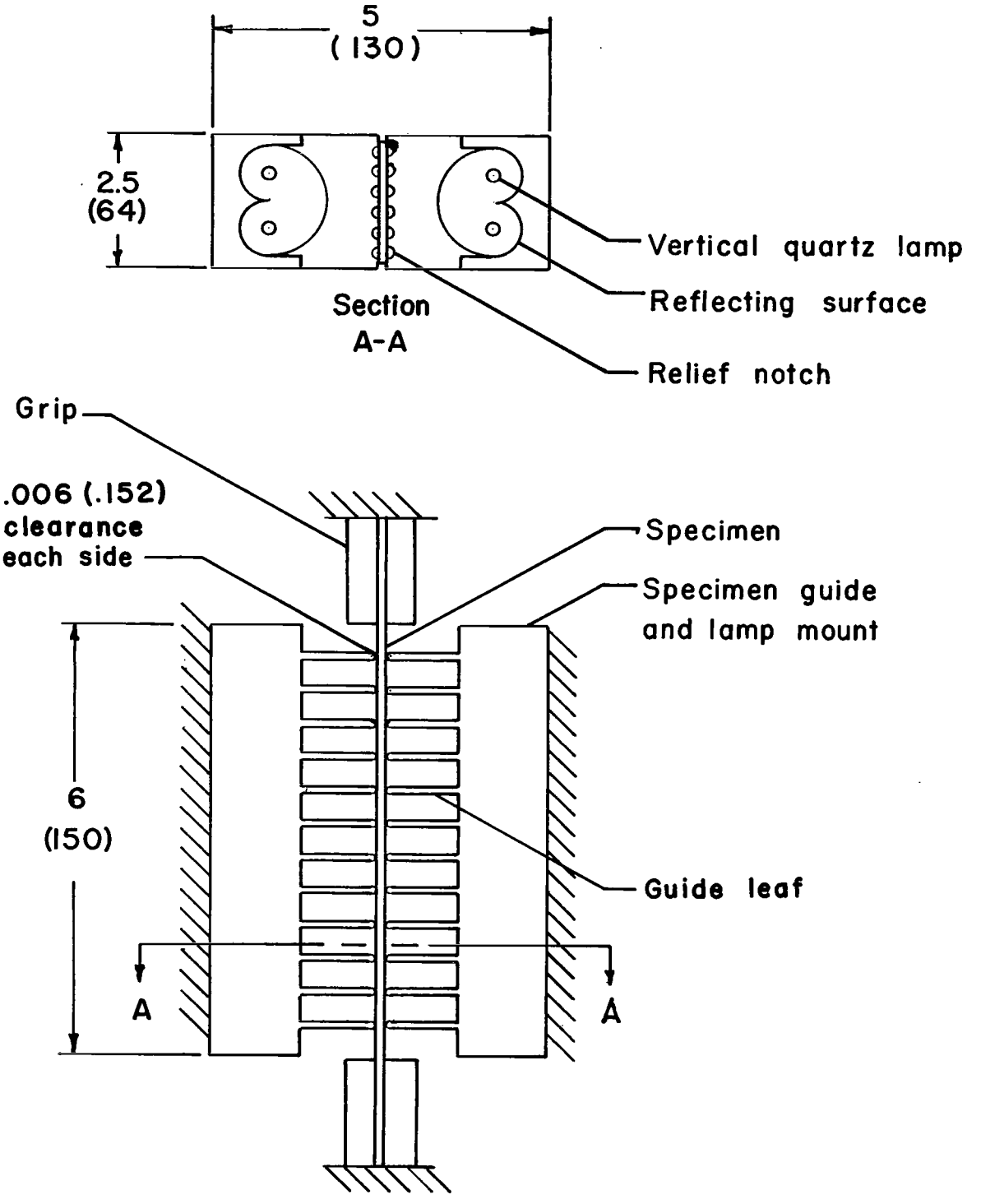

Figure 9.- Diagram of specimen support and heater. (Dimensions are in inches with millimeter equivalents in parentheses. Diagram is not to scale.)

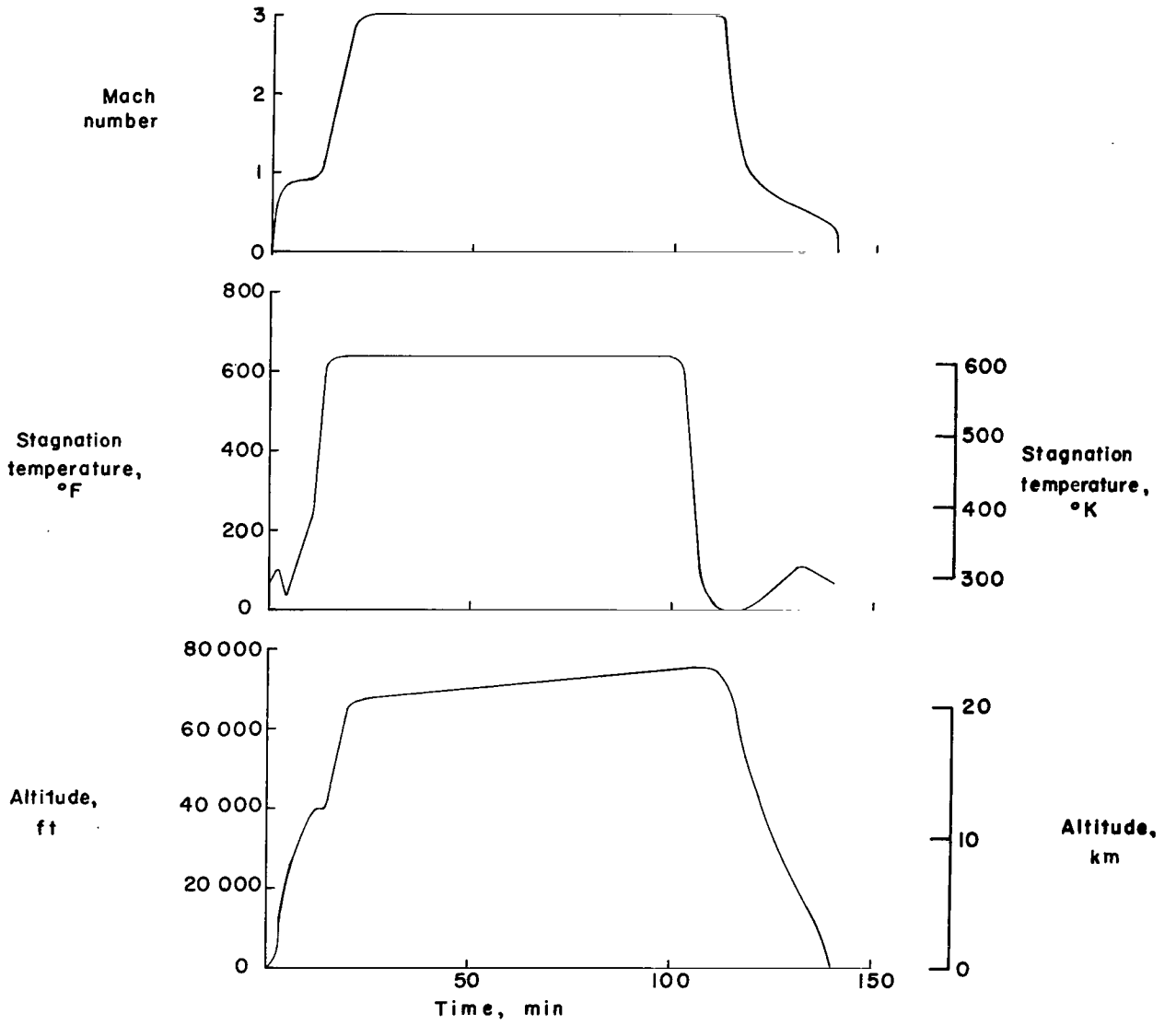

Figure 10.- Assumed flight profile.

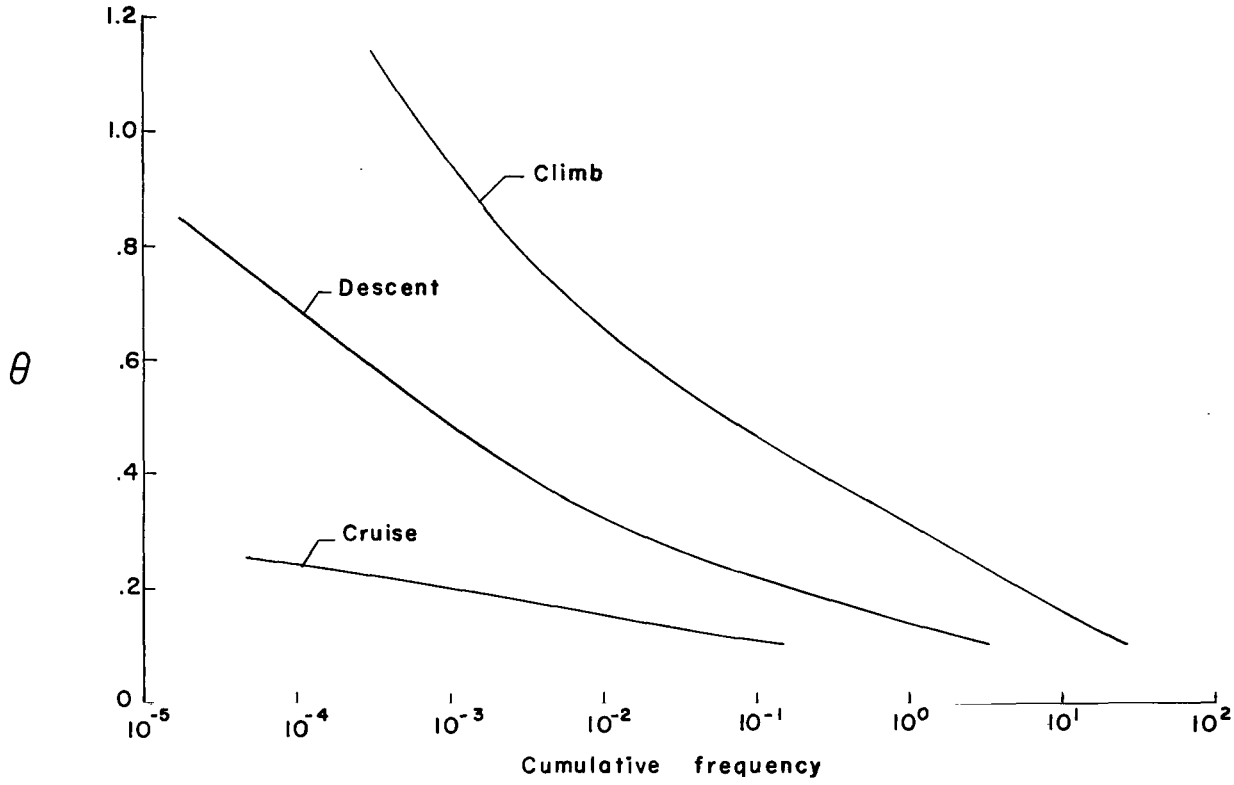

Figure 11.- Derived cumulative frequency of occurrence of θ per flight for gusts.

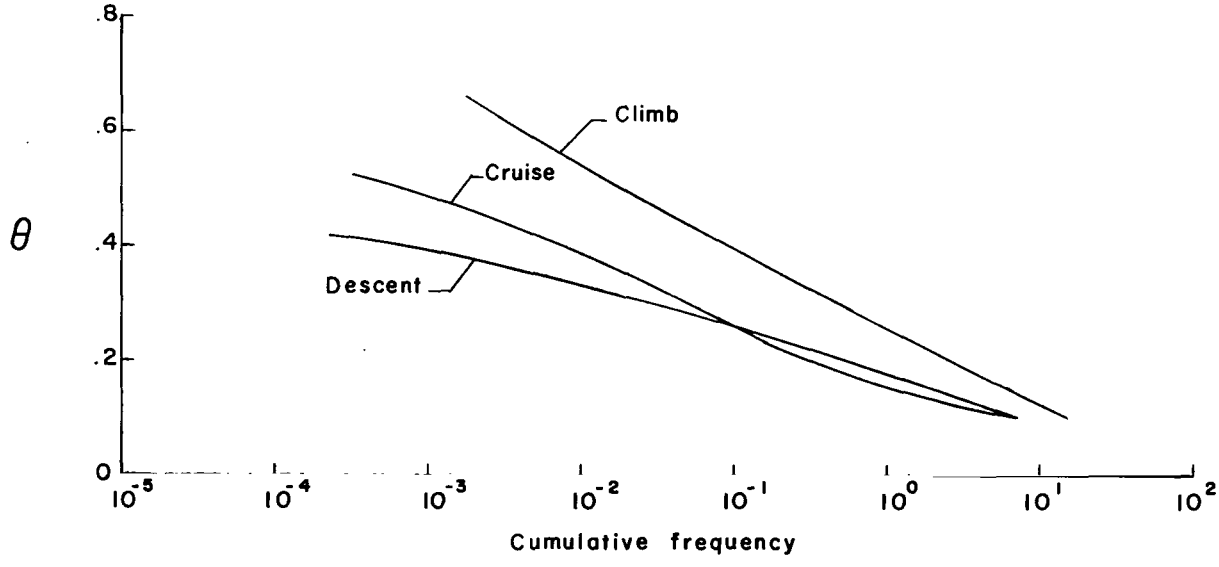

Figure 12.- Cumulative frequency of occurrence of θ per flight for operational maneuvers.

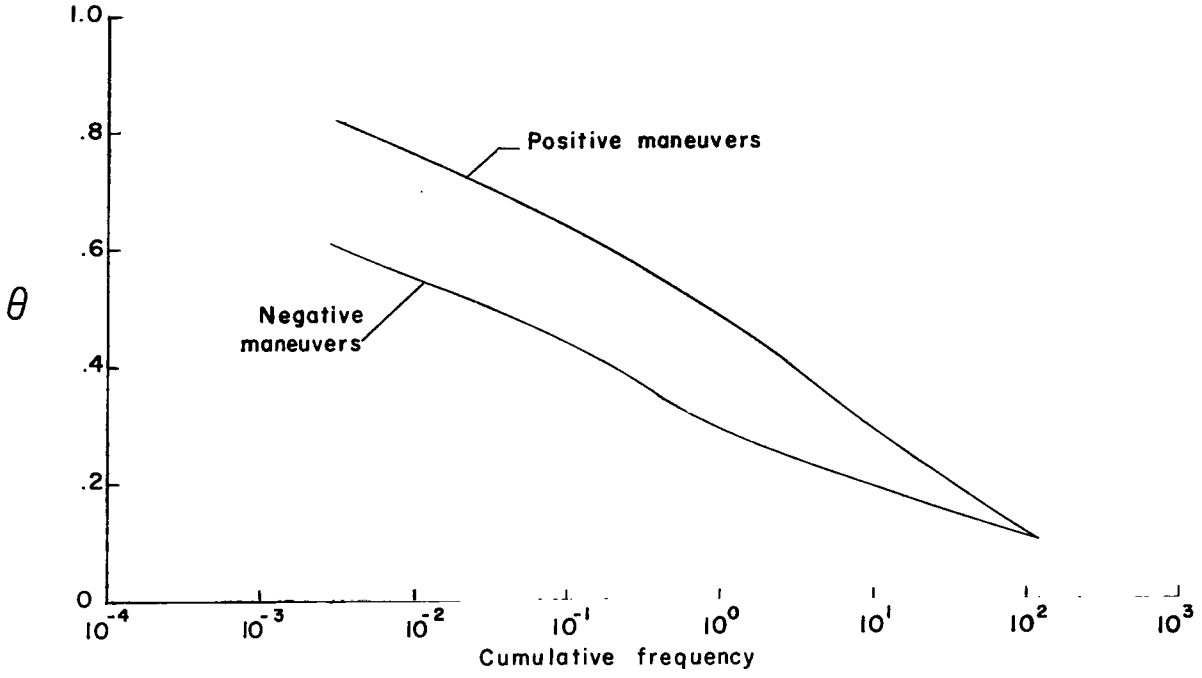

Figure 13.- Cumulative frequency of occurrence of θ per flight for check-flight maneuvers.

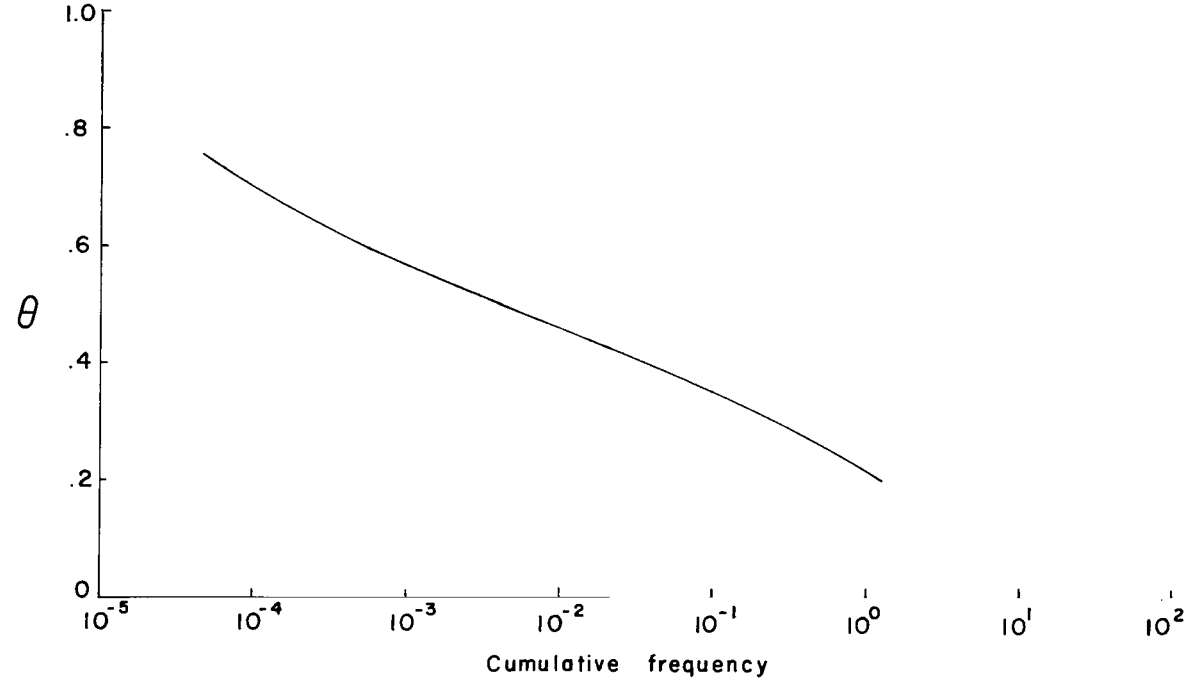

Figure 14.- Cumulative frequency of occurrence of θ per flight for taxiing (used only in test type B).

NASA-Langley, 1969 —— 32 L-6248

"The aeronautical and space activities of the United States shall be conducted so as to contribute . . . to the expansion of human knowledge of phenomena in the atmosphere and space. The Administration shall provide for the widest practicable and appropriate dissemination of information concerning its activities and the results thereof."

—NATIONAL AERONAUTICS AND SPACE ACT OF 1958

NASA SCIENTIFIC AND TECHNICAL PUBLICATIONS

TECHNICAL REPORTS: Scientific and technical information considered important, complete, and a lasting contribution to existing knowledge.

TECHNICAL NOTES: Information less broad in scope but nevertheless of importance as a contribution to existing knowledge.

TECHNICAL MEMORANDUMS: Information receiving limited distribution because of preliminary data, security classification, or other reasons.

CONTRACTOR REPORTS: Scientific and technical information generated under a NASA contract or grant and considered an important contribution to existing knowledge.

TECHNICAL TRANSLATIONS: Information published in a foreign language considered to merit NASA distribution in English.

SPECIAL PUBLICATIONS: Information derived from or of value to NASA activities. Publications include conference proceedings, monographs, data compilations, handbooks, sourcebooks, and special bibliographies.

TECHNOLOGY UTILIZATION PUBLICATIONS: Information on technology used by NASA that may be of particular interest in commercial and other non-aerospace applications. Publications include Tech Briefs, Technology Utilization Reports and Notes, and Technology Surveys.

Details on the availability of these publications may be obtained from:

SCIENTIFIC AND TECHNICAL INFORMATION DIVISION

NATIONAL AERONAUTICS AND SPACE ADMINISTRATION

Washington, D.C. 20546